Logistical Capacity Frictions and Trade*

Kashish Arora† Mohit Saharan‡ Shekhar Tomar§
CUHK *ISB* *ISB*

April 18, 2026

Abstract

We provide a novel physical mechanism, *logistical capacity frictions*, to explain inertia in trade adjustment following large tariff shocks. Using transaction-level data, we find that the rerouting of Chinese goods through Mexico, a "CapEx-light" margin involving minimal processing, remains negligible for 2.5 years after the 2018 US-China trade war, despite immediate tariff incentives. We identify a corridor-level bottleneck—border warehousing capacity—as the primary driver of this delay. Rerouting scaled only in 2021, once a multi-year construction pipeline delivered new warehousing capacity. Therefore, the speed of trade reallocation is bounded by the localized capacity of logistics infrastructure at the margin.

JEL Codes: F13, F14, R42

Keywords: logistics, capacity frictions, rerouting, trade war, warehousing, tariffs

*We thank Konrad Adler, Shilpa Aggarwal, Emilio Bisetti, Gianluca Benigno, Thomas Chaney, Dave Donaldson, Jan Fransoo, Pranav Jindal, Myrto Kalouptsidi, John Leahy, Alejandra Martinez, Sebastian Mitraille, Dilip Mookherjee, Nikolay Osadchiy, Martin Rotemberg, Amit Seru, Hanu Tyagi, Venky Venkateswaran, Lei Ye and conference participants at the European Winter Meeting of the Econometric Society, and the Annual Conference on Economic Growth and Development for helpful comments and suggestions. All errors are our own.

†CUHK Business School, Hong Kong. Email: kashisharora@cuhk.edu.hk

‡Indian School of Business, India. Email: msaharan96@gmail.com

§Indian School of Business, India. Email: shekhar_tomar@isb.edu

1 Introduction

The broad international consensus favoring free trade has fractured considerably over the past decade. The US–China trade war that began in 2018 marked a sharp departure from the post-World War II trend toward deeper global integration (Colantone et al., 2022; Irwin, 2020).[1] However, we know far less about the dynamics of supply-chain adjustment in response to such large policy shocks. In this paper, we focus on the 2018 imposition of Section 301 tariffs by the US on China to understand the dynamics of supply-chain adjustment. While the tariffs triggered an immediate contraction in bilateral US–China trade, we find that the reallocation of these flows to third countries, such as Mexico, lagged by several years. Recent work (Boehm et al., 2023) documents that this lag is a systemic feature as trade elasticities are substantially lower in the short-run relative to the long-run. To explain this divergence, existing mechanisms typically emphasize firm-side frictions, such as the time required to install productive capacity or search for new trade partners. In contrast, we identify a distinct physical channel: *logistical capacity frictions*, which can prevent short-run trade response. We show that even when price arbitrage incentives are immediate, the supply of logistics infrastructure, notably warehousing and cross-docking facilities, is inelastic in the short term. Consequently, the trade reallocation is delayed by the multi-year gestation lags in logistical capacity expansion.

To isolate this channel, we examine the *rerouting* of Chinese goods via Mexico during the 2018 US–China trade war. This setting offers a unique forensic laboratory for three reasons. First, the large magnitude of the tariff shock created sufficient incentives to reconfigure trade flows. Second, rerouting is primarily an *operational adjustment*, involving transshipment and minimal processing, rather than a reallocation of production. Because this margin should respond quickly to tariff incentives, any delay in rerouting is unlikely to reflect the capital investment needed to expand manufacturing capacity and instead points to external logistical

[1] A growing body of work has documented the bilateral effects of these policies (Amiti et al., 2019; Cavallo et al., 2021; Chang et al., 2021) and their spillovers to bystander countries (Fajgelbaum et al., 2024).

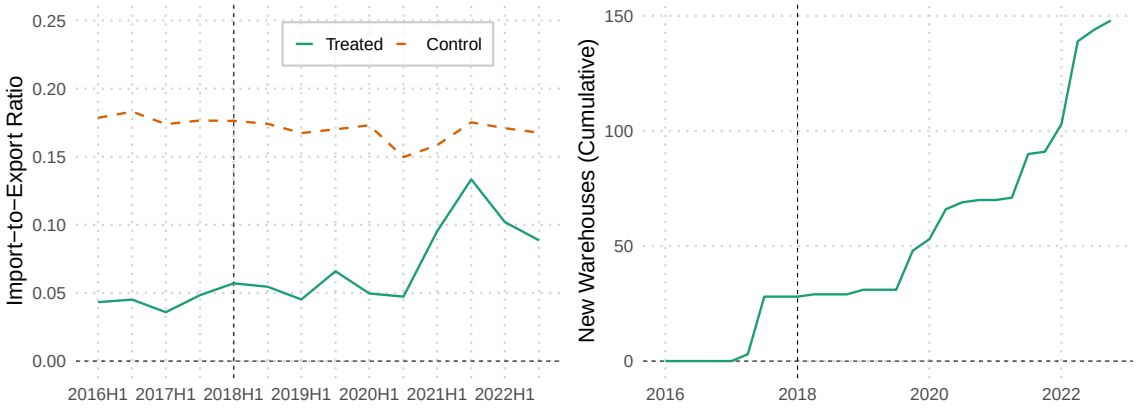
constraints. Third, Mexico is a natural conduit for such activity because it is the principal land gateway for US trade and is deeply integrated into North American supply chains.

Figure 1 provides motivating evidence for our hypothesis by highlighting the temporal synchronization between trade flows and infrastructure delivery. Panel (a) plots the ratio of Mexico's import value from China to its export value to the US, computed separately for the products targeted by the Section 301 tariffs (treated) and those not targeted (control). This ratio serves as a diagnostic for intermediation: If firms use Mexico to reroute Chinese products to the US, the import-to-export ratio should rise following the tariff shock for the treated group. Strikingly, the treated ratio remains flat for nearly three years after 2018 and increases sharply beginning in 2021, driven by a rapid rise in China-to-Mexico imports relative to Mexico-to-US exports. In contrast, the control ratio is remarkably stable over time, indicating stability in trade intensities for nontargeted products. Panel (b) reports new warehousing capacity delivered near the major ports of entry in US border counties. Deliveries accelerate only in late 2020, immediately preceding the spike in the treated trade ratio. Because these facilities provide essential cross-docking and logistics support required on the US side of the border, the synchronized timing is suggestive of a locally binding logistics bottleneck that delayed short-term trade adjustment. The remainder of the paper provides granular microevidence on rerouting dynamics and mechanism tests, triangulating independent data sources to discipline both the timing and the location of the logistics bottleneck.

To quantify rerouting, we use granular bill of lading data from S&P Panjiva, which covers more than 160 million unique transactions. We construct a comprehensive firm-product-quarter panel covering the whole universe of Mexican trade, specifically tracking exports to the US and imports from China between 2016 and 2022. We match these data with product-level tariff information from Bown (2021). Our core analyses focus on products included in the first tariff tranche, implemented in 2018-Q3.

We begin by developing a stringent test to identify the rerouting of Chinese goods through Mexico. We focus on intrafirm rerouting, which provides the most transparent measurement

Figure 1: Logistical Capacity Frictions and the Delayed Adjustment of Trade



(a) Import-to-Export Ratio (b) Increase in Border Warehousing

Notes: Panel (a) plots, by half-year, the ratio of Mexico's import value from China to its export value to the United States. The treated group includes HS 8-digit products targeted by the US Section 301 tariffs on imports from China, implemented in 2018-Q3; the control group includes all other HS 8-digit products. Trade data are from Panjiva (S&P Global). Panel (b) plots the cumulative number of newly added warehousing units in five major US border counties that serve as ports of entry for US-Mexico trade. The series is constructed from OpenStreetMap features labeled as "warehouse". The warehouses provide logistics and cross-docking facilities on the US side of the border. The vertical dashed line marks 2018-H1, the pre-tariff period.

of rerouting identifiable using trade data. Specifically, our test flags cases where a Mexican firm's imports from China are matched to its subsequent exports to the US at the HS 8-digit product and quarter level. Such within-firm-product, same-quarter import-export matches are difficult to reconcile with standard production timelines; they instead capture rapid turnaround and minimal processing prior to re-export.[2] A key advantage of this measure is that it isolates trade flows requiring minimal firm-level capital expenditure, "CapEx-light". Documenting a delayed response even in this CapEx-light margin provides a sharp test for external logistics frictions being the primary bottleneck, rather than internal firm-level frictions.

Beyond temporal matching, we apply a value-added filter, classifying transactions as rerouting only when implied domestic value-added falls below a conservative 20 percent threshold, a benchmark consistent with entrepôt hubs like Hong Kong (Feenstra and Hanson, 2004).[3] Applying this filter yields a conservative lower bound on rerouting activity and further

[2]Mexican firms can serve as conduits for rerouting Chinese goods to the US to arbitrage tariffs through multiple channels. We discuss these various channels in Section 5.1.

[3]Our results are robust to using alternate thresholds for value addition.

sharpens the timing evidence by focusing on the most CapEx-light adjustment margin.

We then use a difference-in-differences (DiD) strategy that exploits product-level variation in US tariffs to isolate rerouting dynamics. Specifically, we compare outcomes for tariffed and nontariffed HS 8-digit products within the same HS 4-digit category before and after the trade war. Using our value-adjusted measure, we find that rerouting in tariffed products increases by approximately 75 percent relative to the pre-shock baseline. Crucially, the event study estimates mirror the aggregate timing observed in Figure 1: firm-level rerouting is statistically indistinguishable from zero in the immediate post-tariff period before exhibiting a sharp, nonlinear surge in 2021.

We translate the estimated rerouting response into dollar-denominated trade volumes and the associated loss in tariff revenue. The rerouting of tariffed products rises by USD 300 million per year in 2021–2022, corresponding to an estimated USD 75 million in annual fiscal leakage for the US Treasury. Because our measurement focuses on intrafirm, same-product value-adjusted rerouting, these estimates represent a conservative lower bound. Overall, this channel alone accounts for 4.8 percent of the total increase in Mexico's imports of tariffed products from China in 2021–2022, or an equivalent 13.6 percent of the pre-period imports of these tariffed goods into Mexico.

We next establish that the observed adjustment lag is driven by logistical capacity frictions at the US–Mexico border. We first document that logistical capacity is a first-order input mandated by institutional constraints: Because Mexico–US trade is overwhelmingly truck-borne and US regulations restrict Mexican carriers to narrow commercial zones near ports of entry, goods must be cross-docked and transferred from Mexican to US carriers at the point of entry (Frittelli, 2014). This mandate renders trade flows structurally dependent on the localized supply of border warehousing. We show that this capacity reached an operational floor in 2018, with vacancy rates in major ports-of-entry areas falling to stock-out levels (below 5 percent), and relaxed only in early 2021 after the new supply materialized, reflecting the standard gestation delays associated with the planning and construction of commercial

real estate (Glancy et al., 2026). The delivery of this capacity in 2021 coincided with an immediate surge in rerouting and warehouse absorption, suggesting that physical logistics had previously throttled the trade response.

To isolate the logistical channel, we conduct a series of tests to rule out competing explanations. We first test the search friction hypothesis by examining "pipeline firms," or prior rerouters, that have already incurred the fixed costs of operating on the China–Mexico–US corridor before the trade war. If partner-search frictions were the main source of delay, pipeline firms should respond earlier than other firms. Instead, they exhibit the same adjustment lag as other firms. This similar delay pattern is difficult to reconcile with partner-search frictions as the dominant source of delay.

We then localize the friction along the China–Mexico–US corridor by comparing the timing of trade adjustment on the upstream and downstream legs. Upstream China–Mexico imports begin to rise in 2020 for firms that were already sourcing from China into Mexico but had not previously shipped onward to the US. In contrast, pipeline firms—those already active on the full corridor—do not expand imports until 2021, when rerouting itself begins to rise. On the downstream leg, Mexico–US exports remain flat for all firms until 2021. Taken together, these patterns show that direct imports into Mexico could adjust earlier, whereas rerouted shipments could not, pointing to a bottleneck on the Mexico–US leg.

Furthermore, consistent with a binding border-capacity constraint, the physical dimension of shipments shapes the timing of adjustment. Space-efficient products—proxied by low shipment volume and weight—witness expanding exports in 2020-H2, whereas higher-footprint products adjust later and more weakly. Taken together, the upstream-downstream timing wedge and the footprint-based sequencing of exports point to a binding constraint downstream—at the Mexico–US border—rather than upstream sourcing constraints.

Next, we investigate the boundary conditions of this logistical channel by determining the thresholds under which rerouting becomes economically viable. Specifically, we show that while logistical frictions govern the timing of adjustment, the initial decision to reroute

depends on the magnitude of the arbitrage opportunity. We demonstrate this by evaluating the rerouting response of products targeted in mid-2019, which faced a significantly lower tariff of 7.5 percent compared to the 25 percent tariff levied on products targeted in 2018-Q3. In sharp contrast to our baseline results, we find no evidence of rerouting for these lower-tariff products. This discontinuity implies that rerouting becomes viable only when the arbitrage wedge is large enough to offset the compliance and transaction costs associated with navigating logistical bottlenecks.

To formalize these conditions, we develop a model in which rerouting requires a minimum arbitrage wedge to be viable. This threshold-based response is consistent with Madsen et al. (2025), who show that high ad valorem rates incentivize firms to exploit informational blind spots in customs enforcement. These patterns also suggest that the United States–Mexico–Canada Agreement (USMCA) is unlikely to be the primary driver of our results. Because the USMCA tightened rules of origin (RoO) and raised compliance costs for claiming preferential treatment, it made minimal-processing intermediation less attractive. Consistent with this interpretation, we find that rerouting is concentrated in products with low "Most Favored Nation" (MFN) duties, for which firms can pay the standard rate and bypass the costly USMCA certification process altogether. Combined with the corridor-specific timing evidence above, it also makes broad contemporaneous shocks, such as COVID-19, unlikely to account for the delayed rerouting response.

Our paper makes three contributions. First, we provide a novel physical mechanism—logistical capacity frictions—to explain the inertia in trade adjustment following a large tariff shock. While a growing literature documents significant production reallocation towards beneficiaries such as Vietnam and Mexico after the US–China trade war (Alfaro and Chor, 2023; Utar et al., 2025; Lee and Rhee, 2025), the structural factors governing the speed of this transition remain less understood. We show that even when price arbitrage incentives materialize immediately, trade reallocation is constrained by the inelastic short-term supply of logistical infrastructure. This physical bottleneck also provides a granular microfoundation

for the well-documented gap between short- and long-term trade elasticities (Boehm et al., 2023; Drozd et al., 2021; Ruhl et al., 2008). Our mechanism is distinct from existing theories that attribute slow adjustment to a firm's internal sunk costs, such as capital-reallocation frictions (Lanteri and Rampini, 2023; Blonigen, 2002) or the search for new trade partners (Chaney, 2014). By documenting how external logistical constraints bind, we demonstrate that a country's ability to capitalize on trade shocks depends as much on localized corridor capacity as it does on comparative advantage. Critically, because the supply of corridor capacity is determined by independent developers rather than the trading firms themselves, the bottlenecks we identify are fundamentally external to the exporter's span of control. Consequently, unlike internal firm-level frictions, these logistical constraints are trade-policy-invariant, creating a bottleneck that imposes a systemic ceiling on the speed of trade adjustment and delays optimal firm-level response.

Second, we contribute to the literature on trade-related infrastructure by identifying logistical capacity frictions arising from the short-term inelasticity and limited reallocation of private border logistics assets. Traditional work in the geography of trade emphasizes how public infrastructure—roads, ports, and railroads—reduces trade costs and expands market access in the long run (e.g., Ducruet et al., 2024; Allen and Arkolakis, 2022; Donaldson and Hornbeck, 2016).[4] While standard transportation frictions can often be mitigated in the short run through route substitution or mode choice (Brancaccio et al., 2024, 2020; Fajgelbaum and Schaal, 2020), we demonstrate that border-specific logistical inputs are fundamentally more rigid. Because facilities like warehousing and cross-docking terminals are highly localized and governed by multiyear commercial leases, they do not permit the rapid reallocation characteristic of shipping or trucking markets.[5] More broadly, our findings suggest that

[4]This literature generally treats infrastructure as a permanent feature of the landscape that enables spatial price arbitrage (Aggarwal and Chatterjee, 2025; Allen and Atkin, 2022; Donaldson, 2018).

[5]Recent work by Brueckner and Rosenthal (2025) and Gupta et al. (2022) documents the frictions in the commercial real estate market due to long-term lease contracts, averaging approximately 6–7 years. In the industrial and warehousing sector, these contracts are predominantly structured as triple net (NNN) leases, where the tenant assumes responsibility for all property-related operating expenses, taxes, insurance, and maintenance, in addition to base rent. With vacancy rates at an operational floor in 2018, this lease structure precludes the reallocation of existing capacity, rendering the border warehousing contractually inelastic.

similar logistical capacity constraints may bind and prevent rapid trade reallocation after large trade shocks as capacity cannot expand in the short run. Consequently, trade volumes may remain capped until new logistics supply is delivered.

Finally, we advance the forensic measurement of trade rerouting and regulatory arbitrage. While preliminary evidence of "China-washing" has been documented at the product level (Freund, 2025; Liu and Shi, 2019) and the transaction level (Iyoha et al., 2025), we provide the first systematic characterization linking rerouting to firm capability, product attributes, and the magnitude of the tariff wedge. In addition, we advance the methodology for identifying rerouting in transaction-level trade data. We demonstrate that standard firm-product matching can overstate rerouting by a factor of five. By applying a stringent value-added filter, we isolate a conservative annual rerouting flow of USD 300 million in the China–Mexico–US corridor. This granular insight reveals that a significant portion of the post-tariff trade surge reflects regulatory arbitrage rather than shifts in fundamental comparative advantage. Crucially, we document that this arbitrage response was contingent upon the expansion of corridor-specific logistical infrastructure. In our setting, this response is not frictionless: It scales only when corridor-specific logistics capacity expands. Because this capital is characterized by high asset specificity, it represents a substantial sunk-cost risk. The economic value of this capacity is inherently policy-contingent, depending upon the persistence of the tariff wedge and the prevailing enforcement regime.

2 Data

We construct our analysis sample using two datasets: international bill of lading data from S&P Panjiva, and product-level tariff data from Bown (2021).

2.1 S&P Panjiva Shipment-Level Data

We use shipment-level trade data from S&P Panjiva, which compiles information from customs declarations and bills of lading (BoL) for Mexico. Each record includes information on trading partners (firm name, identifier, and address, etc.), shipment date, HS 8-digit product code, trade value (USD), and quantity.

For baseline analyses, we use Mexico's imports from China and exports to the US from 2016 to 2022. We use Mexican export data for three reasons. First, while Mexican records provide actual transaction values, Panjiva's US data requires price imputation for calculating shipment value.[6] Second, the Mexican data cover all transport modes (road, rail, air, and sea), while the US import data is restricted to maritime shipments (Schafhäutle and Sran, 2024), thereby omitting the bulk of overland trade between US and Mexico. Consistent with this comprehensive coverage, we find that our aggregated shipment-level data closely tracks the dynamics of Mexico's trade with the US and China in the official UN Comtrade statistics (Appendix Figure A.1). Finally, Chinese trade data are not available in the S&P Panjiva universe for the period after 2018.

We aggregate the data to the firm-product (HS 8-digit) quarterly level. Our regression sample focuses on persistent trade relationships, retaining firm-product pairs that appear for at least four quarters during the analysis period to remove incidental transactions.[7] Table 1 (Panel A) reports the summary statistics for our final sample. The panel spans 32 quarters, covering 21,034 firms and 8,473 HS 8-digit products in the exports sample and 28,360 firms and 8,776 HS 8-digit products in the imports sample.

Finally, most Mexico-US exports are overland, by road. Appendix Table A.1 reports the modal breakdown: truck shipments account for more than 90 percent of transactions and more than 70 percent of shipment value, and this split is stable across the periods. This high

[6] See Flaaen et al. (2023) for a comprehensive evaluation of S&P Panjiva imputation for the US. Other studies leveraging this data include Ganapati et al. (2024) for US transit trade and Bruno and Shin (2023) for the Mexican context.

[7] This filter retains a substantial share of overall trade value: 98% of exports and 95% of imports.

reliance on road transport makes the corridor especially dependent on border warehousing and cross-docking capacity, aligning closely with our focus on logistical capacity frictions.

Table 1: Summary Statistics

Panel A: Summary of Mexican Trade Data		
	Exports (US)	Imports (China)
	(1)	(2)
# Transactions	14,182,338	9,296,447
# Unique Firms	21,034	28,360
# Unique Products	8,473	8,776
# Unique Firm × Products	228,709	482,584
Mean: Firm Trade (USD Million)	0.408	0.049
Panel B: Trade in Tariffed Products		
	2016-2017	2021-2022
# Unique Products	186	132
# Unique Firms	3,827	4,460
# Unique Firm × Products	6,263	7,480
Exports US (USD Billion)	40.59	61.34
Imports China (USD Billion)	2.19	8.42
Panel C: Pre-period Mean of Main Outcomes		
	Mean	Std Dev
Ex-Im	0.11	0.32
Ex-Im_{1Y}	0.13	0.34
RR^A	0.07	0.25
RR^S	0.07	0.24

Notes: This table provides summary statistics for the Mexican firm-level trade data used in our analysis. The sample is based on shipment-level bill of lading data from S&P Panjiva (2016–2022). Panel A reports baseline dimensions for the analysis sample. Values are aggregated at the firm × product (HS 8-digit) × quarter level. Panel B focuses on the subset of HS 8-digit products targeted by the 2018-Q3 US Section 301 tariffs against China. Statistics in Panel C are reported as annual averages. Panel C reports means for the primary outcome variables before the trade war (2016-Q1 to 2018-Q2). *Ex-Im* is a binary indicator that takes the value one for simultaneous import from China and export to US within the same firm-product-quarter, else zero. $Ex\text{-}Im_{1Y}$ is an indicator that utilizes the previous year window for imports from China. RR^A and RR^S denote the adjusted and smoothed rerouting measures, respectively, calculated using a 20 percent domestic value-added threshold ($\theta = 0.2$).

2.2 Tariff Data

We use product-level tariff data from Bown (2021), which compiles HS 10-digit US tariffs on Chinese imports. The dataset is constructed from official sources, including announcements from the Office of the US Trade Representative and the US International Trade Commission.

Our main analysis focuses on three major tariff tranches: July 6 (USD 34 billion), August 23 (USD 16 billion), and September 24 (USD 200 billion), all implemented within the third quarter of 2018. This timing allows us to define a consistent treatment period at the quarterly level, with targeted products experiencing a cumulative 25 percent tariff increase.

We aggregate the tariff data to the HS 8-digit level to match our quarterly customs transactions, yielding a final panel of more than 6.5 million firm-product-quarter observations, covering approximately 21,000 unique firms and 228,000 firm-product pairs. Following the implementation of the US tariffs on China, trade patterns for the targeted products shifted dramatically. The value of treated products exported from Mexico to the US increased from USD 41 billion in 2016–2017 to USD 61 billion in 2021–2022 (Panel B in Table 1). More strikingly, imports of these products from China increased from USD 2.2 billion to USD 8.4 billion.

While the US targeted approximately 6,800 products in 2018-Q3, Panel B shows that the arbitrage response is concentrated in a specific subset of goods. Among the targeted products, only 186 products see active trade in the pre-period; following the trade war, this narrows to 132 unique HS 8-digit products. This reduction suggests a consolidation of arbitrage activity into specific high-volume product lines. The observed import response is mainly driven by differentiated consumer and industrial goods, such as electronics and automobiles. Appendix Table A.2 provides a detailed breakdown of the major tariffed product categories imported by Mexico during the 2021—2022 period.

3 Empirical Strategy

In this section, we describe our main estimation strategy. We evaluate the impact of tariff changes on multiple outcomes: Mexican exports to the US, Mexican imports from China, and measures of trade rerouting. We examine a panel of Mexican firms $f \in \mathcal{F}$, transacting in products $p \in \mathcal{P}$ at the HS 8-digit level, over quarters $t \in \mathcal{T}$. Let Y_{fpt} denote the quarterly

outcome variable for firm f, product p, and quarter t. Each product p belongs to a broader HS 4-digit category, denoted by $\tilde{p} \in \tilde{\mathcal{P}}$.

We estimate the following difference-in-differences (DiD) based event study specification:

$$Y_{fpt} = \phi + \sum_{\tau=\text{2016-H1}}^{\text{2022-H2}} \gamma_\tau \left(Treat_p \times \mathbb{1}_{t=\tau} \right) + \delta_{fp} + \delta_{\tilde{p}t} + \varepsilon_{fpt}, \tag{1}$$

where $Treat_p$ is an indicator set to one if product p is subject to US tariffs on Chinese imports in 2018-Q3, else zero. $\mathbb{1}_{t=\tau}$ is an indicator equal to one for half year τ and zero otherwise. The coefficient γ_τ captures the differential impact on tariffed products in period τ relative to the baseline year 2017. Since we are interested in trade dynamics, the above equation directly gives us the event study estimates. Errors ε_{fpt} are clustered at HS 8-digit product level.

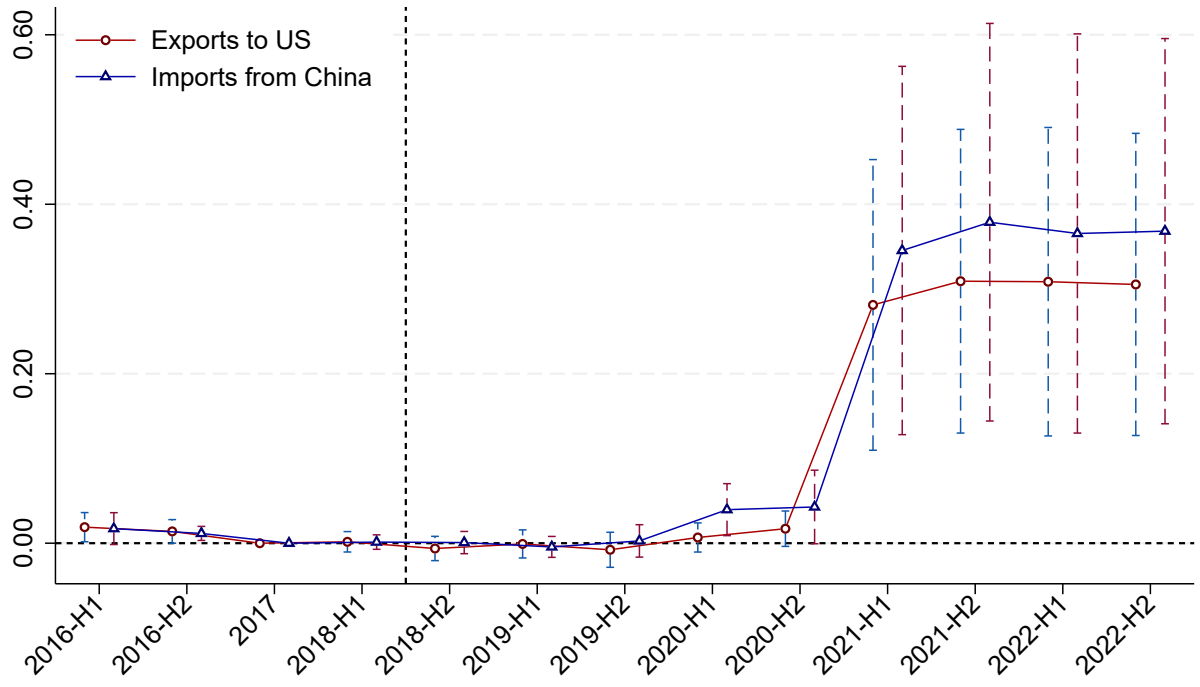
We include a rich set of fixed effects. First, firm×product fixed effects, δ_{fp}, control for time-invariant characteristics specific to each firm-product pair, such as firm size and firm-product quality. Second, product (HS 4-digit)×quarter fixed effects $\delta_{\tilde{p}t}$ control for time-varying shocks common to the broader HS 4-digit category, such as global price changes or demand shifts. In essence, our specification compares the outcomes for tariffed products before and after 2018-Q3, against changes in nontariffed products within the same HS 4-digit category $\tilde{p}$. We mainly use the above specification since all the tariffed products in this tranche witnessed the same effective 25 percent tariff increase, however, we report estimates for tariff elasticity as robustness.

A distinctive feature of our empirical design is the restriction of the comparison group to tariffed and nontariffed products within a single destination. This design avoids the potential violations of the Stable Unit Treatment Value Assumption that arise when "rest-of-world" trade flows at HS 8-digit product level serve as the control group, which may be directly influenced by the trade diversion effects of the US–China trade war (Fajgelbaum et al., 2024). Our approach minimizes the effect of such spillovers.

4 Impact of Tariffs on Firm-Level Trade Flows

We first estimate the impact of tariffs on Mexican firms' trade. Figure 2 reports the event-study estimates for the probability of exporting tariffed products to the US and importing them from China. There are no significant pre-trends before the trade war. Subsequently, both exports and imports exhibit minimal change in the period immediately after the tariff imposition. However, the magnitude of the impact grows substantially from 2021. The probability of exports to the US increases by 30 percentage points, and the probability of imports from China increases by 37 percentage points by 2022. We report the corresponding impact on trade value and quantity in Appendix Figure A.2, which reveal identical dynamics.

Figure 2: Event Study: Impact of Tariffs on Mexican Firms' Trade



Notes: The event study plot gives the impact on Mexican firms' trade (exports to the US and imports from China) for products targeted by the 2018 US Section 301 tariffs. The outcome variable is an indicator equal to one if firm-product-quarter exports to the United States (imports from China) are positive, and zero otherwise. Regressions are at the firm × product (HS 8-digit) × quarter level. All regressions include HS-4 × Quarter-Year and Firm × HS 8-digit fixed effects. Standard errors are clustered at the HS 8-digit level, and 95 percent confidence intervals are shown.

Overall, Mexican firms' exports to the US and imports from China increase for tariffed

products beginning 2021. We find a muted response immediately after tariff escalation and then a nonlinear jump in trade. However, some of this delay may be due to time needed to scale manufacturing, so we focus on CapEx-light trade flows, i.e. rerouting, in the next sections to isolate the effect of logistical capacity constraints.

5 Evidence of Delayed Rerouting Response

In this section, we first outline our methodology for measuring trade rerouting, then provide a dynamic response of rerouting through Mexico.

5.1 Construction of Rerouting Measures

Figure 3 illustrates four ways in which Mexican firms can reroute Chinese exports to the US. In Case A, a Mexican firm imports an HS 8-digit product x from China and exports the same product to the US following light processing in Mexico. In Case B, a firm imports a product x from China and exports a different product y to the US. Cases C and D involve multiple-firm chains in which imports and exports are handled by separate entities. Data limitations, specifically the absence of comprehensive domestic supply-chain linkages in Mexico, prevent us from empirically tracking Cases C and D. Consequently, we focus on Case A, which offers the cleanest identification of rerouting. Because this restriction excludes interfirm transfers and transformations across HS codes, our results provide a conservative lower bound on the aggregate incidence of rerouting. We also extend our analysis to incorporate Case B in Section 5.2.

To characterize the extensive margin, we construct two rerouting indicators: (i) $Ex-Im_{fpt} = \mathbb{1}\{\text{Imported}_{fpt} > 0 \wedge \text{Exported}_{fpt} > 0\}$, which equals one if firm f imported and exported the same HS 8-digit product p in quarter t and (ii) $Ex-Im_{1Y,fpt} = \mathbb{1}\{\text{Exported}_{fpt} > 0 \wedge (\exists t' \in \{t-3,\ldots,t\} : \text{Imported}_{fpt'} > 0)\}$, which equals one if the firm exported product p in quarter t and imported the same product in the current quarter or any of the three preceding

Figure 3: Trade Rerouting Through Mexico: Four Cases

	Same Product	**Alternate Product**
Intrafirm	A	B
Interfirm	C	D

Notes: This figure presents four cases of trade rerouting through Mexico, classified according to whether imports from China and exports to the United States are handled within the same firm (intrafirm) or across different firms (interfirm), and whether the product exported to the United States is the same as or different from the product imported from China. In all cases, the intermediary firms are located in Mexico.

quarters. $Ex-Im$ provides a stringent definition of rerouting as it requires simultaneous imports and exports within the same firm-product-quarter, allowing very limited time for processing or transformation. $Ex-Im_{1Y}$ represents a less restrictive definition, as it relaxes the timing constraint and allows more time for value addition.

We next define rerouting measures on the intensive margin. As a first pass, consider a simple measure, the Unadjusted Rerouting Ratio (URR), based on the overlap between imports and exports:

$$RR^{U}_{fpt} = \frac{\min(E_{fpt}, I_{fpt})}{E_{fpt}} \tag{2}$$

where E_{fpt} (I_{fpt}) is the export (import) value of firm-product fp in quarter t to the US (from China). Iyoha et al. (2025) uses a similar measure to identify rerouting. This measure works well when import and export values are of similar magnitude. However, when export value substantially exceeds import value (indicating high domestic value addition by Mexican intermediary firm), RR^{U}_{fpt} spuriously classifies genuine export activity as rerouting. For instance, if a firm exports USD 100 to the US, but imports only USD 50 from China, $RR^{U}_{fpt} = 0.5$. Thus, despite the high value addition (50 percent), the unadjusted measure incorrectly flags this case as 50 percent rerouting.

To overcome such issues, we define adjusted measures that explicitly account for value

addition. We proceed in two steps. First, we define the lower bound on value-added share as:

$$VA^{\text{lb}}_{fpt} = \begin{cases} 0, & \text{if } E_{fpt} = 0 \text{ and } I_{fpt} = 0, \\ \max\left\{0,\ \dfrac{E_{fpt} - I_{fpt}}{E_{fpt} + \epsilon}\right\}, & \text{otherwise.} \end{cases}$$

where the ratio $\dfrac{E_{fpt} - I_{fpt}}{E_{fpt} + \epsilon}$ denotes the value-added share of exports, and ϵ is a small positive constant to avoid division by zero.[8] We subsequently define the adjusted rerouting measure as:

$$RR^{A}_{fpt} = \max\left\{0,\ 1 - \frac{VA^{\text{lb}}_{fpt}}{\theta}\right\} \times Ex - Im_{fpt}, \tag{3}$$

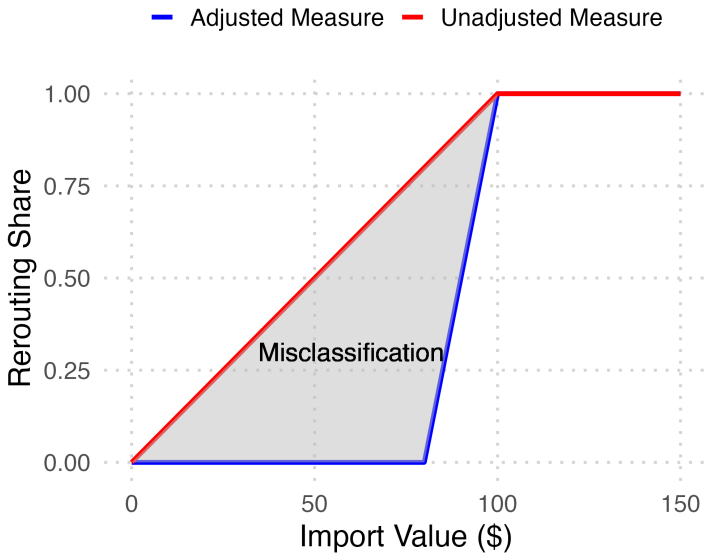
where $\theta \in (0, 1]$ is a threshold for the domestic value-added share: shipments with $\text{VA}^{\text{lb}}_{fpt} \geq \theta$ are classified as nonrerouted. For the above example, where RR^{U}_{fpt} equals 0.5, the adjusted measure RR^{A}_{fpt} assigns a value of 0 (i.e. no rerouting), since $\text{VA}^{\text{lb}}_{fpt} = 0.5$ exceeds the threshold $\theta = 0.2$. For our baseline empirical analyses, we set $\theta = 0.2$, a 20% cutoff. This threshold is conservative (similar to entrepôt hubs in (Feenstra and Hanson, 2004)), as it classifies any flow with domestic value added exceeding 20 percent as genuine export activity.[9]

Figure 4 demonstrates misclassification as a function of import value for a fixed export value of USD 100 and $\theta = 0.2$. The red line corresponds to RR^{U}_{fpt} and assigns a nonzero rerouting value for all cases except when imports equal zero. The blue line represents RR^{A}_{fpt}, which takes a value of zero for cases with large $E_{fpt} - I_{fpt}$, implying a significant value addition. The shaded area highlights the misclassification region, representing cases where the unadjusted measure incorrectly flags genuine value-added exports as rerouting.

[8] In our context, the term "value added" denotes the domestic value retention by Mexican firms, measured as the gross margin between exports and imports. This differs from the standard macroeconomic definition, which subtracts all intermediate inputs to calculate value addition. However, this definition is conservative precisely because the differential $(E_{fpt} - I_{fpt})$ captures not only physical value addition but also markups and intermediary costs such as domestic transport or regulatory fees. By treating the entire gross margin as domestic content, we minimize the risk of falsely classifying genuine high-margin exports as rerouting.

[9] Our results are robust to variations in θ around this threshold.

Figure 4: Illustration of Misclassification in Unadjusted Rerouting Measure



Notes: The figure plots rerouting shares as a function of imports from China under the adjusted and unadjusted rerouting measures. The blue (red) line corresponds to adjusted (unadjusted) rerouting measure RR^A (RR^U). The shaded area corresponds to the cases misclassified as rerouting by the unadjusted measure. Parameter values: Exports to the US = 100 USD, $\theta = 0.2$, and $\epsilon = 0.1$.

Table 2 quantifies the extent of this misclassification in our sample. We find that 38 percent of the observations have $RR^A_{fpt} = 0$ but $RR^U_{fpt} > 0$, which means that the unadjusted measure incorrectly flags low import cases as rerouting. A small intermediate segment (2.76%) has $0 < RR^A_{fpt} < 1$ while $RR^U_{fpt} > 0$; here, both measures flag rerouting, but the unadjusted measure overestimates its extent by an average share difference of 0.39. For the remaining 59 percent of the cases, both measures converge to a value equal to one.

Finally, to avoid sharp discontinuities at the threshold, we propose a smoothed rerouting measure RR^S_{fpt}:

$$RR^S_{fpt} = \frac{1}{k} \log\left(1 + \exp\left(k \cdot \left(1 - \frac{VA_{\text{smooth}}}{\theta}\right)\right)\right) \times Ex - Im_{fpt}. \tag{4}$$

where the parameter k governs the sharpness of the transition and VA_{smooth} is a smooth approximation to VA^{lb}_{fpt}. Qualitatively and quantitatively, RR^S_{fpt} behaves similarly to RR^A_{fpt}, assigning zero values for cases with high value addition. Appendix Section C.1 provides

additional details on the construction and properties of this measure.

Table 2: Extent of Misclassification in Unadjusted Rerouting Measure

Segment	Percentage (1)	Mean Difference (2)
$RR^A_{fpt} = 0$ & $RR^U_{fpt} > 0$	38.00	0.19
$0 < RR^A_{fpt} < 1$ & $RR^U_{fpt} > 0$	2.76	0.39
$RR^A_{fpt} = 1 = RR^U_{fpt}$	59.24	0

Notes: This table quantifies the extent of misclassification in the unadjusted rerouting measure relative to the adjusted rerouting measure in our sample of firm-product-quarter exports to the United States and imports from China. The sample is restricted to observations for which the unadjusted measure, RR^U_{fpt}, indicates positive rerouting. In Row 1, the unadjusted measure (RR^U_{fpt}) flags rerouting while the adjusted measure (RR^A_{fpt}) does not. In Row 2, both measures indicate rerouting but differ in magnitude. Row 3 reports observations for which $RR^A_{fpt} = RR^U_{fpt} = 1$. Column 1 reports the share of observations in each category, and column 2 reports the mean difference between the two measures.

Rules of Origin (RoO) and Legal Feasibility: One concern regarding rerouting is the legal feasibility of re-exporting Chinese goods via Mexico without violating strict RoO conditions under the free trade agreement (FTA) between the US and Mexico. While the FTA imposes rigorous regional value content requirements, often exceeding 50 percent, these constraints bind only if firms seek preferential duty-free access (Burfisher et al., 2019). Firms can legally bypass Section 301 tariffs *without* meeting these strict thresholds by opting to pay the standard US Most Favored Nation (MFN) tariff. In fact, the compliance costs under strict RoO are substantial, leading many firms to utilize MFN rates to avoid administrative burdens even under normal trade conditions (Conconi et al., 2018). Consistent with this incentive, Appendix Figure A.3 shows that the vast majority of rerouted products in our sample face MFN rates below 5 percent. The resulting arbitrage opportunity, paying a small MFN duty to avoid the 25 percent tariff, renders the rerouting strategy profitable.

5.2 Dynamics of Rerouting through Mexico

We estimate Equation 1 for various rerouting measures and report the event study estimates in Figure 5. Panel (a) shows the impact on extensive margin, and Panel (b) shows the

impact on value-adjusted measures. We observe no significant pre-trends before the trade war. Notably, we find that rerouting is negligible in the period immediately following the trade war and does not intensify until 2021. Subsequently, the coefficient estimates for 2021 and later periods become positive and significant for all rerouting measures. For RR^A, the coefficient estimates are around 0.053, suggesting a (0.053/0.07 =) 75 percent increase in rerouting in 2021 over the baseline period (Panel C in Table 1). Since the dynamics are very similar for RR^S, we focus on the RR^A measure for the remaining analyses.

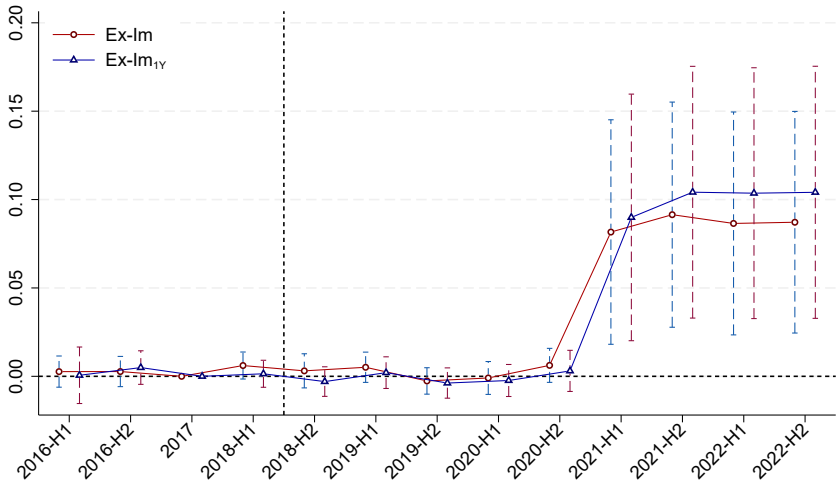
The delayed surge in rerouting until 2021 aligns with the necessary lead time for infrastructure investment, mirroring the sharp acceleration in border warehousing documented in Section 6.1. While this period also coincides with the implementation of the USMCA, which replaced the North American Free Trade Agreement (NAFTA), and COVID-19, several factors ensure our identification isolates the tariff effect. We defer the discussion of these potential confounding factors to Section 6.5.

We also report simple DiD estimates in Appendix Table A.3. For the extensive-margin indicator $Ex-Im$, the treated products exhibit significantly more rerouting in the post period, with a 3.7 percentage point increase. The one-year measure $Ex{-}Im_{1Y}$ shows a similar pattern, with a slightly larger coefficient of 4.3 percentage points, as expected for this less restrictive measure. Columns (3) and (4) report results for the value-adjusted measures. Both the adjusted (RR^A) and smooth (RR^S) measures show a significant increase in rerouting intensity following the trade war. The coefficient for the adjusted measure is 0.022 and is very similar for the smooth measure.[10]

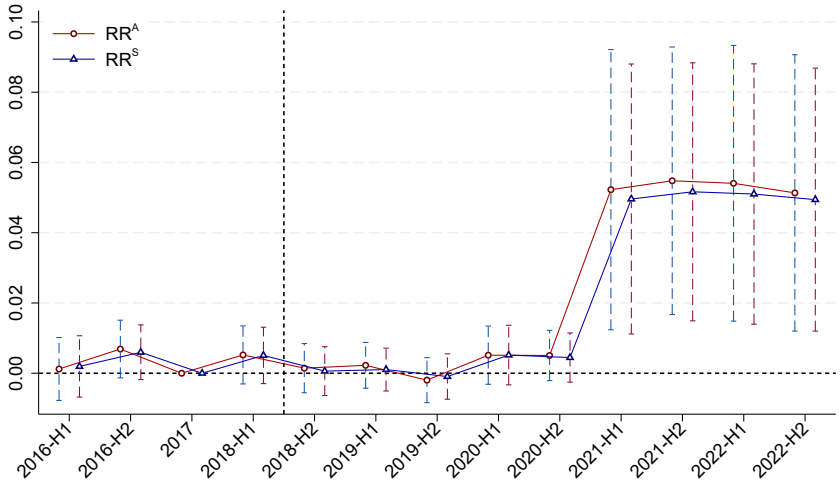
A note on the lower bound of rerouting: Our estimates represent a conservative lower bound on the rerouting activity for two reasons. First, our rerouting measures focus on *intrafirm* and not *interfirm* rerouting. Second, we impose a stringent value-addition threshold that classifies shipments with substantial domestic value added as nonrerouted,

[10]Appendix Table A.5 reports results using the unadjusted measure. While estimates remain positive and significant, they are considerably larger in magnitude, implying that failure to correct for misclassification substantially overstates the increase in rerouting following the trade war. See Section 7 for further discussion.

Figure 5: Dynamics of Rerouting through Mexico



(a) Extensive Margin



(b) Value-Adjusted Measures

Notes: The event study plot gives the impact on rerouting through Mexico for products targeted by the 2018 US Section 301 tariffs. Panel (a) reports event-study estimates for two extensive-margin measures of rerouting, $Ex-Im$ and $Ex-Im_{1Y}$. Panel (b) reports event-study estimates for two value-adjusted measures of rerouting, RR^A and RR^S. Coefficients are reported relative to the baseline year 2017. Regressions are estimated at the firm × product (HS 8-digit) × quarter level and include HS-4 × quarter-year and firm × HS 8-digit fixed effects. Standard errors are clustered at the HS 8-digit level, and 95 percent confidence intervals are shown.

further tightening our lower bound.

Accounting for "Case B" Rerouting: We test the sensitivity of our results to the inclusion of rerouting under Case B. Specifically, we define an indicator that equals one if a firm exports a tariffed product to the US and imports *any* product from China. Appendix Table

A.4 reports the results, with the outcome variables $Ex{-}Im^{Any}$ ($Ex{-}Im^{Any}_{1Y}$) corresponding to import of any product from China in the same quarter (the last year). We find a positive and significant increase on rerouting in both columns, with coefficient estimates quantitatively similar to the baseline $Ex{-}Im$ indicator in Appendix Table A.3. These results suggest that Case B represents a less prominent form of rerouting, in case of within intrafirm rerouting.[11]

Quantity Rerouting: In our baseline specification, we control for differential trends in sectoral prices through HS 4-digit product × quarter fixed effects, thereby accounting for broader changes in sectoral prices. Therefore, our value-based results reflect changes in trade quantity. However, we provide more direct evidence of quantity rerouting. For each firm-product-quarter, our outcome variable is defined as the share of quantity rerouted:

$$RR^{Q}_{fpt} = \frac{\min\{E^{Q}_{fpt},\, I^{Q}_{fpt}\}}{E^{Q}_{fpt}} \times \mathbb{1}(RR^{j} = 1), \tag{5}$$

where E^{Q}_{fpt} and I^{Q}_{fpt} are export and import quantities, and $\mathbb{1}(RR^{j} = 1)$ is an indicator equal to one if the value-based rerouting measure $RR^{j} \in \{RR^{A},\, RR^{S}\}$ equals one, else zero. Unlike the value-added rerouting measure for trade value, an analogous measure cannot be defined for quantities. We therefore interact the quantity share, $\frac{\min\{E^{Q}_{fpt}, I^{Q}_{fpt}\}}{E^{Q}_{fpt}}$, with $\mathbb{1}(RR^{j} = 1)$ to ensure that high value-added cases are classified as zero quantity rerouting. Table A.6 reports the estimates. The coefficient estimates on the interaction terms are positive and significant from 2021 onwards, confirming that the increase in rerouting is driven by quantity flows.

Product-Level Determinants of Rerouting: We examine how product attributes shape selection into rerouting. We focus on two key characteristics: (i) product differentiation and (ii) demand elasticity. For differentiated goods, preserving specific brand attributes or variety may justify the higher costs of rerouting through Mexico. Conversely, for products with

[11]The two outcome variables $Ex{-}Im^{Any}$ and $Ex{-}Im^{Any}_{1Y}$ do not utilize input-output tables to isolate relevant inputs for the export of tariffed products. If we account for specific input linkages, the difference in pre-period mean level of rerouting between these measures and $Ex{-}Im$ would be even smaller.

highly elastic demand, firms are more likely to substitute toward alternative countries rather than navigating the additional costs and delays associated with rerouting through Mexico.

To test these predictions, we use product-level differentiation (Rauch, 1999) and elasticity measures (Fontagné et al., 2022) as interaction terms in our regressions. Appendix Table A.7 reports the results. Rerouting is more pronounced for differentiated products: The triple interaction term is positive and statistically significant in columns (1) and (3). In contrast, the interaction with elasticity is negative but small and statistically insignificant in both measures (columns (2) and (4)), providing limited evidence that demand elasticity strongly predicts selection into rerouting in our data. Overall, rerouting is concentrated in more differentiated product categories, consistent with the view that firms are willing to incur the additional logistics costs of rerouting when preserving the underlying variety is especially valuable.

5.3 Robustness

Continuous Treatment: We replace the baseline specification, which uses an indicator for tariffed products, with a continuous treatment measure equal to the 25 percent tariff rate. These estimates yield the tariff elasticity. These results are reported in Appendix Table A.8 and are consistent with our baseline results.

Alternate Thresholds for Value Addition (θ): We test the sensitivity of our results to alternative value-added thresholds. The results remain robust for $\theta = 0.15$ and $\theta = 0.25$, as shown in Appendix Table A.9.

US as the Main Export Destination: Our baseline rerouting measures combine firms' total imports from China with their exports to the US. One concern is that Chinese inputs may be used in the production of goods exported to destinations other than the US. In such cases, the baseline measures could capture the use of Chinese intermediates in export production more generally, rather than rerouting to the US. This concern is less likely in our context,

given that the US accounts for more than 80 percent of Mexican exports. Nevertheless, we restrict the sample to firm-product pairs with at least 80 or 90 percent of their export revenues from the US. This restriction excludes cases where Chinese inputs may be used for exports to third countries. The results remain similar (Appendix Table A.10).

Comparison Within Narrow Product Categories: Our baseline estimates compare tariffed products to nontariffed products within the same HS 4-digit category. As a robustness check, we narrow the control group by restricting to products within the same HS 6-digit category. The results remain similar, as reported in Appendix Table A.11.

Section 232 Steel and Aluminum Tariffs: To ensure that our results are not confounded by the temporary US tariffs on Mexican steel and aluminum (June 2018–May 2019), we exclude affected products from the sample. Appendix Table A.12 reports similar results.

6 Logistics Constraints and Trade Dynamics

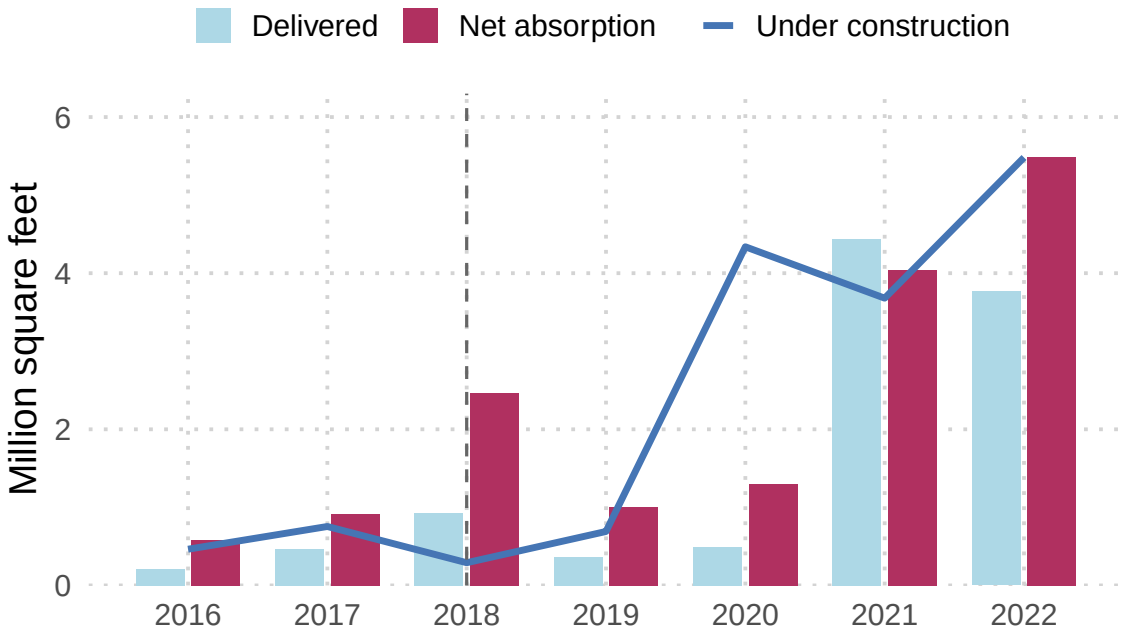
In this section, we demonstrate how logistical capacity frictions govern the dynamics of rerouting. We first establish that the border warehousing capacity reached an operational floor around the 2018 tariff escalation and was only relaxed in 2021 after a multiyear construction cycle. Next, we provide empirical tests showing that the time-varying severity of these physical frictions explains the observed intertemporal response of rerouted trade flows.

6.1 Border Logistics Capacity: Dynamics and Constraints

Spatial Regulation—Commercial Zones: A key characteristic of the US–Mexico corridor is its reliance on road-based transit, which renders trade flows structurally dependent on the warehousing and cross-docking infrastructure located at the border. This infrastructure is not merely a market choice but is spatially anchored by US Department of Transportation regulations. Specifically, the US Department of Transportation restricts Mexican trucks to

operating within 25–50 miles of the border counties, known as commercial zones.[12] This restriction forces Mexican carriers to offload cargo near border crossings, necessitating that cross-docking facilities be concentrated near ports of entry, where goods can be transferred to US carriers for long-haul distribution. Such institutionally constrained transit zones are a common feature of global land-based trade, suggesting that the logistical capacity frictions we identify are a general structural feature of international trade corridors rather than an idiosyncrasy of the North American context (Arvis et al., 2011).

Figure 6: Industrial Real Estate Dynamics in El Paso (2016–2022)



Notes: The lightblue and maroon bars represent annual totals for delivered construction (supply) and net absorption (realized demand) respectively, measured in millions of square feet. The solid line represents the volume of industrial space under construction (the pipeline), also in millions of square feet. The vertical dashed line denotes 2018, marking the onset of the US–China trade war. Source: CBRE Industrial MarketView Reports, hand-collected and compiled by the authors.

Logistics—Short-Term Supply Inelasticity: To document the capacity constraints governing the trade response, we hand-collected industrial market data from CBRE reports for

[12]The Federal Motor Carrier Safety Administration (FMCSA) manages operating requirements for Mexico-domiciled motor carriers. See Commercial zone definition and Title 49 for details on commercial zone rules. Most commercial zones allow Mexican trucks to operate within a 25-mile radius of counties where US Customs and Border Protection facilities are located. Frittelli (2014) provides detailed information on Mexican truck operations in the US.

El Paso (Texas), a major port of entry at the border. Figure 6 tracks three key series—total square footage of industrial real estate under construction, its deliveries, and net absorption. The data collectively confirm that border capacity reached an operational floor in 2018, followed by a delayed expansion. The figure establishes three facts. First, space under construction rose sharply after 2018—from a baseline of 0.5 million square feet in 2016 to a peak of 4.3 million square feet in 2020—indicating rapid investment. Taken together, the deliveries in 2021 and 2022 add approximately 8.2 million square feet of new capacity, representing a massive 18 percent expansion of El Paso's total pre-trade-war warehouse stock (44.7 million square feet) in just two years. Second, despite an early investment response, the multiyear gestation lag inherent in commercial construction meant that this new capacity only materialized as a delivery spike in 2021. Finally, net absorption closely tracks new deliveries throughout 2021 and 2022. The fact that newly delivered warehousing (totaling 4.7 million square feet in 2021 alone) is utilized almost immediately after completion shows a significant pent-up demand for trade-related warehousing capacity that was previously throttled by physical infrastructure shortages.

The existence of this logistical bottleneck is further validated by industrial vacancy rates. Relative to a long-term US industrial vacancy benchmark of approximately 6 percent, vacancy rates in major ports of entry plummeted below 4 percent between 2018 and 2020, signaling that the infrastructure was operating at, or near its physical limit.[13] This inelasticity is reinforced by contractual rigidity: Industrial space is typically leased for 6–7 years and is often under NNN contracts (Brueckner and Rosenthal, 2025; Gupta et al., 2022), limiting tenant turnover and reallocation of space even when vacancy reaches stock-out levels. Unlike transportation, where capacity is mobile and can be reallocated through market-clearing prices (Brancaccio et al., 2020), warehousing capacity near ports of entry is both locally fixed and contractually rigid. This dual rigidity renders the short-term supply of logistical infrastructure markedly less elastic than other trade-related inputs.

[13] In warehousing, vacancy at or below 5 percent is commonly characterized as a "stock-out" (see reports by Prologis and Cushman & Wakefield).

While the sustained low vacancy during the 2018–2020 period underscored the high latent value of expansion, the surge in completions only materialized in 2021. This timing is consistent with standard planning and construction lags: As documented by Glancy et al. (2026); Millar et al. (2016), commercial projects typically require 1.5–2 years for entitlements, design, and financing before physical construction begins, followed by a roughly 12-month build cycle. Taken together, these lags imply that the 2021 delivery surge reflects investment decisions made in 2018–2019, shortly after the 2018 tariff escalation. This gestation structure also mitigates simultaneity concerns: Capacity delivered in 2021 was largely predetermined by permitting, financing, and construction decisions made several quarters earlier, rather than a contemporaneous response to the 2021 trade surge.

Ruling Out General Warehousing Boom: The tightness we document is highly localized near ports of entry and does not reflect broader industrial market conditions in Texas, the primary gateway for US–Mexico trade. Appendix Figure A.4 provides a spatial placebo check by comparing El Paso to the Texas state average. Panel (a) shows that vacancy in El Paso falls to stock-out levels by 2019 and remains low through 2022, whereas vacancy in the average Texas market remains substantially higher. Panel (b) shows the corresponding divergence in delivered construction (indices normalized to 100 in 2016): Deliveries in El Paso skyrocketed to an index value of 2,067 in 2021, compared to a modest 165 for the Texas average. Furthermore, Appendix Figure A.5 shows a sharp rent spike in El Paso in 2019–2020, which is not the case for average rents in Texas. The absence of comparable dynamics in the broader Texas market is consistent with a corridor-specific physical bottleneck at ports of entry rather than a regional construction boom.

Market Dynamics in Other Ports of Entry: We find similar dynamics of extreme market tightness and delayed delivery across the other major ports of entry, including Laredo and Otay Mesa (see Appendix Figure A.6), suggesting that these temporal trends were

a systemic feature of the entire border.[14] We complement the market data with forensic evidence of infrastructure growth using satellite imagery and OpenStreetMap data to provide a granular view of the physical expansion.

Forensic Evidence—Border Infrastructure Boom: We next provide forensic evidence of the logistical transformation after the trade war using satellite imagery. Figure 7 illustrates the expansion of logistics near El Paso's Ysleta Port of Entry. The two panels document the logistics capacity development adjacent to the US Customs and Border Protection facility between 2016 (Panel (a)) and 2022 (Panel (b)). In 2016, the land remains largely undeveloped; by 2022, a dense concentration of newly constructed warehouses and logistics terminals has emerged in immediate proximity to the border. Appendix Figure A.7 provides high-resolution evidence of the intensive utilization of these sites, showing the high density of containers and trucks at newly constructed warehouses. Below, we provide systematic quantitative measures of warehouse growth across major ports of entry.

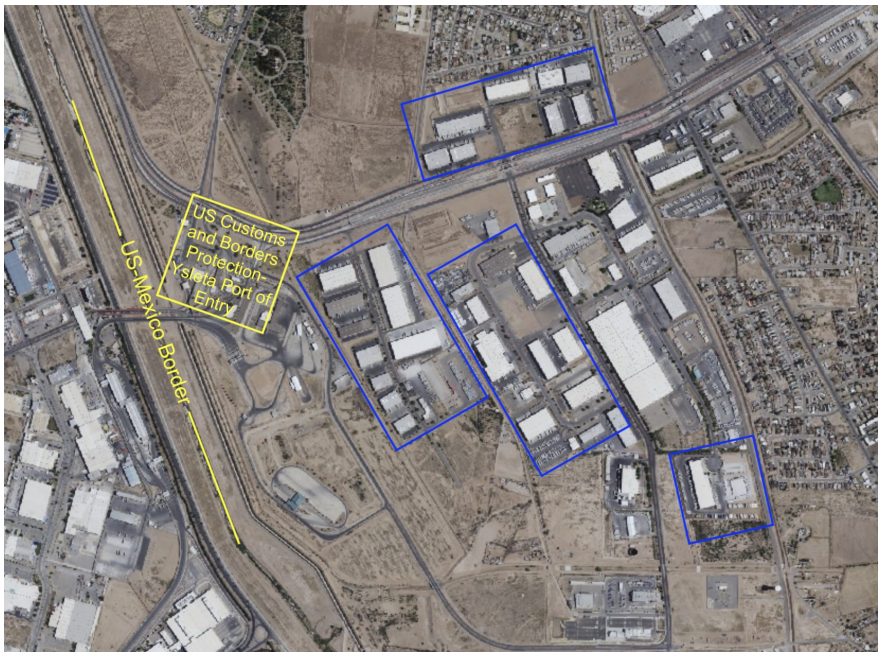
Spatial Identification of Capacity Expansion: We complement the CBRE-based analyses and satellite-based evidence by quantifying the growth in warehousing capacity in five major border counties that handle a significant portion of imports from Mexico. For each county, we compare warehouse growth over time in a near-border treated zone (0–70 km from the US customs office) to a control zone (70–100 km) of comparable area using OpenStreetMap data. Our 70 km threshold is designed to encompass the varying legal definitions of commercial zones. These zones extend beyond a simple population-based radius to include all contiguous municipalities that intersect the port's jurisdiction. By utilizing a 70-km band, we capture the operational catchment area accessible to Mexican-domiciled motor carriers, including neighboring satellite counties that are functionally tied to the port

[14]These series are hand-collected from publicly available CBRE MarketView reports, and coverage is uneven across ports and years. Not all markets report a consistent set of construction deliveries, absorption, and vacancy series in a comparable format. Accordingly, we report city-specific plots for robustness.

Figure 7: Satellite Evidence of Warehouse Development Near El Paso Port of Entry



(a) 2016 (Before Trade War)



(b) 2022 (After Trade War)

Notes: The panels show the US commercial zone adjacent to Ysleta Port of Entry in El Paso, Texas. Panels (a) and (b) give the satellite images from 2016 and 2022, respectively. The highlighted areas in Panel (b) mark new warehousing and logistics facilities that emerged after the onset of the US–China trade war. Map source: National Agriculture Imagery Program (NAIP).

of entry.[15] Appendix Figure A.8 illustrates the construction of these spatial bands.

We track the number of warehouses from 2016 to 2022 using features labeled as "warehouse" extracted from the OpenStreetMap API.[16] Figure 8 plots the cumulative change in the number of warehouses after 2016. We observe a steady increase in the number of warehouses located near the border after 2018, while there is almost no increase in the warehouse count in control areas. This divergence is evident across all major counties.[17] We formally test these patterns using a difference-in-differences specification in Appendix Table A.13. We find a positive and statistically significant interaction term (Post $\times$ Border), indicating that the number of warehouses accelerates disproportionately in the near-border areas after 2018. While control zones see minimal net addition, border zones add an average of 12.5 new warehouses after the tariff escalation. Consistent with the industrial market evidence from CBRE, the near-border warehouse count increases in the period when delivered industrial space begins to rise.

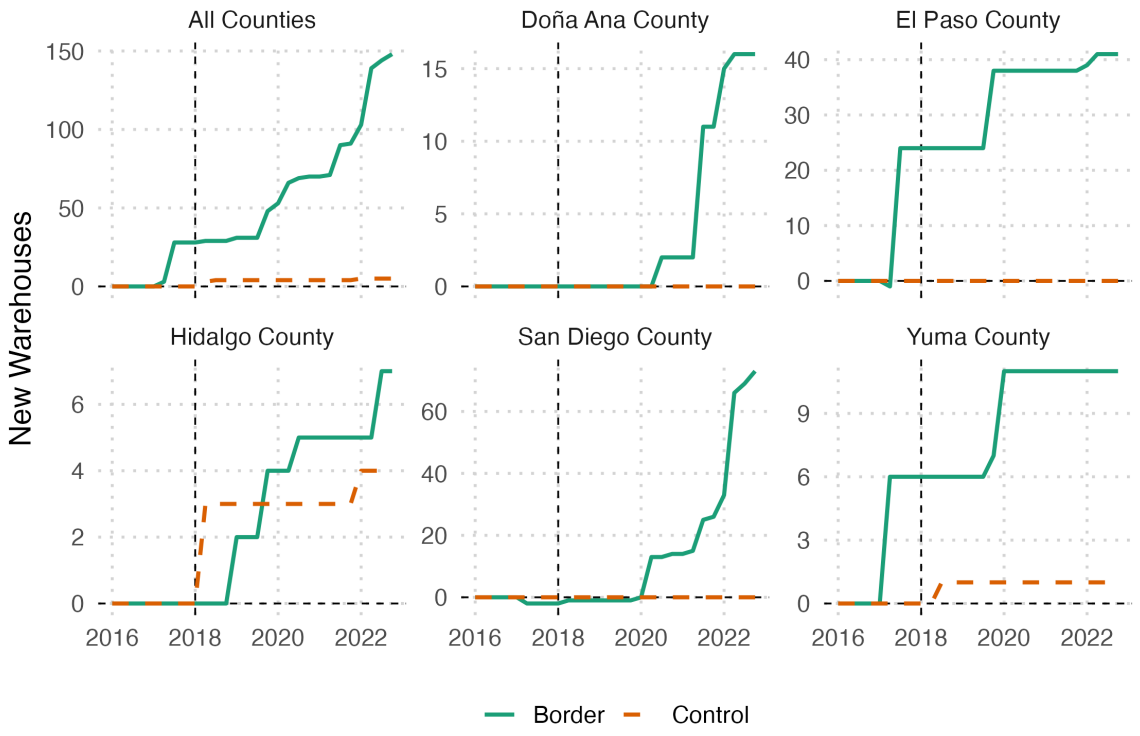
Collectively, these findings document a period of acute short-term supply inelasticity of warehousing in commercial zones after 2018. The confluence of record-low vacancy, regulatory constraints, and contractual rigidity kept logistics capacity at a binding physical floor until the construction cycle delivered new capacity in 2021. We next examine how this time-varying relaxation of border logistics capacity shaped rerouting behavior.

[15]The 70-km threshold is an operational proxy, and not a legal border-commercial-zone boundary. Under FMCSA rules, commercial zones are defined with reference to designated border municipalities. These zones are heterogeneous: some are identified by name, some depend on municipality characteristics, and the rule can extend coverage to contiguous jurisdictions. FMCSA descriptions often refer to border commercial zones as extending about 25 to 50 miles inland, with case-specific expansions. Our 70-km band is meant to capture this broader operational catchment area in a harmonized way across ports.

[16]A potential concern with the OpenStreetMap data is whether the observed increase reflects genuine construction or simply improved mapping coverage. However, this is of minimal concern in our context. First, the warehousing construction data from CBRE broadly align with the expansion of warehousing in OSM data. Second, the absence of a comparable trend in nearby control areas suggests that the results are not primarily driven by an increase in mapping intensity.

[17]The results remain robust when using alternative definitions of spatial bands, with most warehouse growth concentrated in areas near ports of entry.

Figure 8: New Warehouses in Major Commercial Zones (2016–2022)



Notes: This figure plots the cumulative number of new warehouses relative to 2016-Q1 for commercial zone locations within 0–70 km of the border (solid green line) and for a comparison band 70–100 km away (dashed orange line) for major counties that handle Mexico's exports to the US. The two spatial bands have similar area. The "All Counties" panel shows the sum across all the counties in our sample. The vertical dashed line marks 2018-Q2. The five counties in the sample and their primary ports of entry are: Dona Ana County (Santa Teresa); El Paso County (Bridge of the Americas, Ysleta-Zaragoza); Hidalgo County (McAllen-Hidalgo-Reynosa, Anzalduas, Pharr); San Diego County (San Ysidro, Otay Mesa); and Yuma County (San Luis I and San Luis II). Data source: OpenStreetMap. We use the Overpass-turbo API in `R` to get the counts of warehouses in each band.

6.2 Spatial Sorting: Location Choice of Rerouters

One potential explanation for the multiyear delay in rerouting is geographic re-optimization by Mexican firms towards customs offices. Locating closer to customs can reduce trade frictions by improving access to logistics networks and limiting transit and regulatory delays. We assess this mechanism by examining the spatial distribution of rerouting firms relative to Mexican customs offices. Because rerouters manage both the inbound China–Mexico and outbound Mexico–US legs, they have strong incentive to cluster near ports of entry. Motivated by the evidence that exporters sort geographically to minimize trade costs, (Coşar and Fajgelbaum, 2016; Hanson, 1996), we test whether rerouting firms cluster more strongly

around customs locations. Consistent with this corridor-based interpretation, rerouting activity is concentrated in a small set of Mexican gateways connected to the main US border crossings (Appendix Table A.14).

We find that rerouters are located systematically closer to customs offices than the average exporter. Kernel density plots in Appendix Figure C.3 show a sharp left-skew for rerouters. Regression estimates in Appendix Table C.1 show that rerouters are, on average, 50 percent closer to their nearest customs post than nonrerouters. This result is similar when we fix firm locations at their pre-trade-war addresses, confirming that rerouter firms operated from ex-ante optimized locations. Appendix Section C.2 reports the full spatial-sorting analysis.

This spatial selection indicates that rerouting is concentrated among firms already positioned to leverage the corridor at low access costs. The fact that rerouting rises only later in the sample—even for these ex-ante optimized firms—suggests that logistics capacity, rather than firm-side relocation frictions within Mexico, was the binding constraint on rerouting.

6.3 Space Rationing on the Mexico–US Leg

Having ruled out gradual geographic re-optimization within Mexico as the main source of delay, we next ask where the binding friction lies along the rerouting corridor. The key distinction is between the upstream China-Mexico leg and the downstream Mexico-US leg. A clean cross-sectional test based on port-level variation is difficult because capacity constraints were binding across the main border gateways (Section 6.1). With vacancy rates at stock-out levels throughout the corridor, firms had limited scope to avoid the bottleneck by shifting shipments across ports of entry. We therefore rely on time variation and shipment-level volume margins that bear more directly on whether capacity constraints delayed rerouting.

Corridor-Specific Logistic Constraints: First, we provide corridor-specific timing evidence that isolates where the friction binds along the rerouting corridor while holding the tariff-based event-study design fixed. The key question is whether the friction binds upstream

(China → Mexico sourcing) or downstream (Mexico → US exports) in the rerouting corridor. Table 3 reports these tests.

For this test, we define "pipeline firms" (incumbent rerouters) as firms that rerouted at least one product prior to 2018-Q3. These firms have already incurred the fixed costs of establishing the cross-border connections needed to execute rerouting. On the import side, we compare pipeline firms with pre-period experience in the full China → Mexico → US leg to non-pipeline firms that imported from China but did not ship onward to the US. While both groups possess established Chinese sourcing relationships, their import surge timing diverges sharply. Imports for non-pipeline firms increase as early as 2020 (column (2)). In contrast, imports for pipeline firms remain flat until 2021 (column (1)), closely mirroring the delayed timing of the rerouting surge. Because rerouting relies on rapid turnaround, scaling China-Mexico imports in advance would require costly inventory holding in Mexico. Pipeline firms, therefore, have limited incentives to scale upstream imports until downstream Mexico–US shipment capacity can expand. This divergence implies that the bottleneck is not a result of upstream sourcing frictions or aggregate shocks to China-Mexico trade, but is instead specific to the rerouting channel.

On the export side, we compare pipeline firms against other Mexico-US exporters and find no systematic increase through 2020 for both groups operating on the Mexico → US leg of the corridor (columns (3) and (4)).

Taken together, these timing patterns locate the delay downstream in a corridor-level constraint common to firms scaling Mexico → US shipments, rather than on the upstream side, and are consistent with the binding warehousing-capacity constraint.

Evidence of Warehouse Space Rationing: The above corridor timing tests localize the binding friction to the Mexico–US leg, where shipments are structurally dependent on warehousing capacity for staging and cross-docking near ports of entry. This constraint yields a sharp, testable prediction for Mexico-US exports: if border logistics capacity is

Table 3: Locating the Bottleneck on the Rerouting Corridor

Dep. Var	Imported		Exported	
	Pipeline Firm		Pipeline Firm	
	Yes	No	Yes	No
Treat ×	(1)	(2)	(3)	(4)
2016-H1	0.010	0.022^{+}	0.018*	0.023
	(0.007)	(0.012)	(0.008)	(0.019)
2016-H2	0.011^{+}	0.012*	0.017*	0.003
	(0.006)	(0.005)	(0.007)	(0.015)
2018-H1	0.003	–0.000	–0.001	0.003
	(0.006)	(0.005)	(0.007)	(0.011)
2018-H2	0.003	–0.001	–0.004	–0.018
	(0.010)	(0.007)	(0.008)	(0.013)
2019-H1	–0.006	–0.004	0.002	–0.015
	(0.008)	(0.008)	(0.008)	(0.017)
2019-H2	0.005	0.001	–0.005	–0.020
	(0.014)	(0.010)	(0.011)	(0.019)
2020-H1	0.024	0.050**	0.007	–0.002
	(0.016)	(0.018)	(0.009)	(0.021)
2020-H2	0.020	0.059*	0.015	0.017
	(0.019)	(0.024)	(0.012)	(0.022)
2021-H1	0.257*	0.406**	0.246**	0.405**
	(0.104)	(0.119)	(0.091)	(0.098)
2021-H2	0.275**	0.450**	0.275**	0.434**
	(0.107)	(0.131)	(0.093)	(0.109)
2022-H1	0.265*	0.435**	0.273**	0.437**
	(0.108)	(0.130)	(0.094)	(0.110)
2022-H2	0.268*	0.438**	0.270**	0.429**
	(0.105)	(0.126)	(0.092)	(0.108)
Observations	5473216	8034376	4355456	2043076
R-Squared	0.263	0.199	0.293	0.254
HS-4 × QnY FE	✓	✓	✓	✓
Firm × HS-8 FE	✓	✓	✓	✓

Notes: This table reports event-study estimates separately for the China-Mexico and Mexico-US legs of the rerouting corridor. Columns (1)â(2) use an indicator equal to one if a firm imports an HS 8-digit product from China into Mexico in a given half-year. Columns (3)â(4) use an indicator equal to one if a firm exports an HS 8-digit product from Mexico to the US in a given half-year. "Pipeline firms" are firms that operated on the full ChinaâMexicoâUS corridor prior to 2018-Q3, that is, they rerouted at least one product in the pre-period. In columns (2), "non-pipeline firms" are firms with pre-period China-Mexico imports but no onward exports to the US prior to 2018-Q3. In column (4), "non-pipeline firms" are firms with pre-period exports from Mexico to the US but have no imports from China prior to 2018-Q3. Coefficients are reported relative to the omitted baseline year 2017. All specifications include HS 4-digit × half-year fixed effects and firm × HS 8-digit fixed effects. *Treat* indicates HS 8-digit products targeted by the 2018 Section 301 tariffs. Columns (1) and (2) are estimated on the imports sample, while columns (3) and (4) are estimated on the exports sample. Standard errors are clustered at the HS 8-digit level and reported in parentheses. p < 0.01, * p < 0.05, ^{+}p<0.1.

rationed when vacancy is at stock-out levels, then shipments that are less space-intensive should witness early trade adjustment. We therefore split products by pre-period shipment footprint, measured using the median shipment volume at the HS 8-digit level. Because the split is based on pre-period median, it is predetermined and not mechanically driven by post-trade-war changes in shipment footprint.

We estimate the impact on the exported dummy and report the results in Table 4. The results show a clear capacity-rationing pattern: below-median footprint products exhibit an earlier export response (column (2)), including a statistically significant increase already in 2020-H2 that grows thereafter. In contrast, above-median footprint products (column (1)) display weaker and later adjustments. We obtain similar results when footprint is proxied by weight instead of volume (columns (3) and (4)), indicating that the result is not driven by the specific physical metric. This footprint-based asymmetry is consistent with quantity rationing of scarce staging/warehouse space on the Mexico–US leg during the stock-out period.[18]

Separately, we test a complementary prediction about which products expand once capacity begins to loosen. We split products by pre-period value density (value per unit volume or weight) and report the results in Appendix Table A.16. While the footprint split identifies the margin of physical feasibility during the warehousing shortage, the value-density split identifies the margin of economic selection. When vacancy is at stock-out levels, even high willingness to pay cannot translate into higher quantities if capacity is physically unavailable. However, as capacity begins to expand in 2021, high value-density products exhibit a sharp and dominant pickup in exports, whereas low value-density products show minimal response. Together, these two splits provide a consistent forensic evidence: constrained capacity initially forces a rationing that favors low-footprint shipments at the margin, while the subsequent expansion is concentrated in high-value per unit volume products that can bear the high shadow cost of scarce warehousing space.

[18]Here, we use Exported indicator because the test is designed to probe capacity constraints on the downstream Mexico–US leg. Appendix Table A.15 reports analogous estimates using our rerouting measures (Ex-Im and RR^A); these measures are mechanically more restrictive and therefore yield noisier estimates, but the dynamics remain consistent.

Table 4: Space Rationing on the Mexico–US Export Leg

Dep. Var	Exported			
	Pre-Period Volume		Pre-Period Weight	
	High	Low	High	Low
Treat ×	(1)	(2)	(3)	(4)
2016-H1	0.000	0.009	0.001	0.009
	(0.016)	(0.010)	(0.016)	(0.010)
2016-H2	–0.003	0.017	–0.003	0.017
	(0.018)	(0.011)	(0.018)	(0.011)
2018-H1	0.004	0.005	0.005	0.005
	(0.013)	(0.009)	(0.013)	(0.009)
2018-H2	–0.014	0.007	–0.014	0.007
	(0.016)	(0.010)	(0.016)	(0.010)
2019-H1	–0.020	0.016	–0.019	0.016
	(0.018)	(0.010)	(0.018)	(0.010)
2019-H2	–0.037*	0.023	–0.037*	0.023
	(0.018)	(0.014)	(0.018)	(0.014)
2020-H1	–0.013	0.021	–0.012	0.021
	(0.014)	(0.015)	(0.014)	(0.015)
2020-H2	–0.023	0.041**	–0.023	0.041**
	(0.020)	(0.015)	(0.020)	(0.015)
2021-H1	0.104	0.195**	0.104	0.195**
	(0.073)	(0.071)	(0.073)	(0.071)
2021-H2	0.129	0.219**	0.130	0.219**
	(0.080)	(0.074)	(0.080)	(0.074)
2022-H1	0.139^{+}	0.207**	0.139^{+}	0.207**
	(0.077)	(0.070)	(0.077)	(0.070)
2022-H2	0.124	0.213**	0.125	0.213**
	(0.078)	(0.068)	(0.078)	(0.068)
Observations	2445520	3239180	2417016	3267600
R-Squared	0.341	0.324	0.342	0.324
HS-4 × QnY FE	✓	✓	✓	✓
Firm × HS-8 FE	✓	✓	✓	✓

Notes: This table reports event-study estimates for export activity on the Mexico–US leg of the rerouting corridor, separately by pre-period shipment footprint. The dependent variable is an indicator equal to one if a firm exports a given HS 8-digit product from Mexico to the United States in a given quarter. *Treat* indicates HS 8-digit products targeted by the 2018 Section 301 tariffs. Coefficients are reported relative to the omitted baseline year 2017. Columns (1)–(2) split the sample by pre-period shipment volume. For each HS 8-digit product, we compute the median shipment volume across all pre-period observations and classify products as High or Low volume depending on whether this median lies above or below the overall median. Columns (3)–(4) analogously split the sample by pre-period shipment weight. All specifications include HS 4-digit × quarter-year fixed effects and firm × HS 8-digit fixed effects. Standard errors are clustered at the HS 8-digit level and reported in parentheses. p < 0.01, * p < 0.05, ^{+}p<0.1.

6.4 Do Firm-Specific Frictions Explain the Delayed Response?

An alternative explanation for the lag in rerouting response is that firms require time to navigate institutional barriers (legal registration, trade permits), or search for new trade partners. We assess the role of these firm-level frictions by exploiting heterogeneity in prior rerouting experience. Firms with prior export experience tend to form new trade relationships and enter new destinations more quickly than non-exporters (Alvarez et al., 2013).

This heterogeneity provides us a sharp prediction. If firm-specific frictions are the primary source of delayed adjustment, pipeline firms should respond earlier than new entrants following the tariff escalation. In contrast, if logistics capacity frictions are the main binding constraint, the delay should be similar across firms.

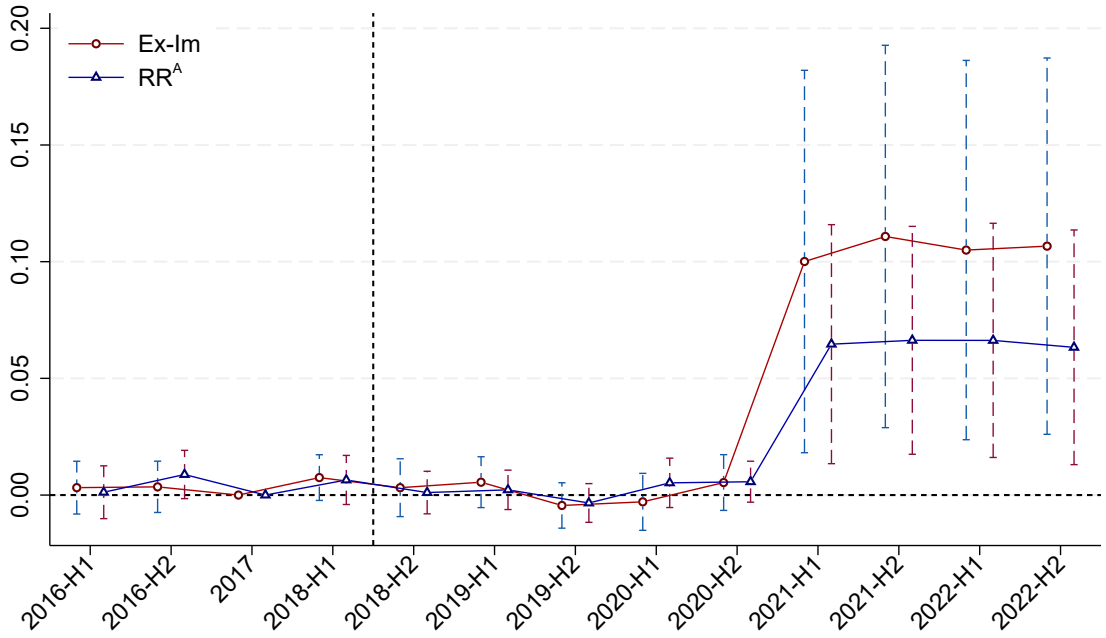
To test this prediction, we estimate rerouting dynamics for pipeline firms separately in Figure 9. Rerouting for these firms remains statistically indistinguishable from zero until 2021, followed by a sharp increase, i.e. no early response. This nonlinear pattern is difficult to reconcile with gradual partner search as the primary friction, which would predict smoother adjustment. These results are consistent with binding logistics capacity constraints that delay scaling even for firms with prior rerouting experience and low entry costs.[19]

6.5 Ruling Out Other Confounders

In this section, we discuss why aggregate shocks, like the COVID-19 pandemic and the implementation of the USMCA, are unlikely to explain the delayed rerouting response. Since our baseline specification controls for HS 4-digit product $\times$ quarter-year fixed effects, we account for any aggregate shocks affecting the broader HS 4-digit product category. For an aggregate shock to explain our findings, (i) it would need to differentially affect targeted HS 8-digit products relative to nontargeted HS 8-digit products within the same HS 4-digit category, and (ii) to do so with timing that matches the rerouting break—an implausibly

[19] Appendix Table A.17 reports the split-sample estimates. The rerouting surge is quantitatively larger among pipeline firms (columns (1) and (3)) than for firms with no prior rerouting experience (columns (2) and (4)).

Figure 9: Dynamics of Rerouting for Pipeline Firms



Notes: This figure reports event-study estimates of rerouting by pipeline firms, defined as firms that rerouted at least one product prior to 2018-Q3. We report estimates for two measures of rerouting $Ex-Im$ and RR^A. Regressions are estimated at the firm × product (HS 8-digit) × quarter level. Coefficients are reported relative to the baseline year 2017. All specifications include HS-4 × Quarter-Year and Firm × HS 8-digit fixed effects. Standard errors are clustered at the HS 8-digit level, and 95 percent confidence intervals are shown.

granular pattern for a broad aggregate shock. Nevertheless, we discuss these candidates directly and show that their timing and scope do not align with the corridor-specific dynamics examined in Section 6.3.

COVID-19: First, the dynamics of rerouting is inconsistent with a pandemic-induced explanation. The US tariffs were implemented in 2018-Q3, six quarters before the onset of the pandemic in 2020-Q1. During this 18-month pre-COVID-19 period, rerouting activity is insignificant, indicating that the delay in adjustment predates the pandemic. Furthermore, the surge in rerouting activity in 2021 materializes precisely when the pandemic in Mexico was at its most severe. As shown in public health data, confirmed COVID-19 cases in Mexico peaked in January and August of 2021.[20] If the pandemic were the primary constraint, we would expect activity to remain depressed during these periods; instead, we observe a

[20]See Our World in Data for the timeline of COVID-19 cases in Mexico.

breakout in rerouting.

Second, this delay is unique to the Mexico–US corridor. Other "bystander" countries, such as Vietnam and Thailand, exhibit a more immediate reallocation of US import sourcing in 2018–2019 following the trade war and well before the onset of COVID-19 (see Figure 2 in Fajgelbaum et al. (2024)). Mexico's delayed response, despite geographic proximity to the US and established trade links with both the US and China, is therefore difficult to reconcile with COVID-19 as the main explanation.

USMCA: Beyond the pandemic, the study period also coincides with the implementation of the USMCA, which replaced NAFTA. However, several factors ensure that our identification isolates the tariff effect. First, unlike NAFTA, the USMCA acted as an institutional headwind; its stricter Rules of Origin and labor value requirements were explicitly designed to discourage nonregional input content. Consistent with this, we find that the vast majority of rerouted products in our sample face US MFN rates below 5 percent, allowing firms to bypass the high administrative and compliance costs required to qualify for preferential treatment under the USMCA (Appendix Figure A.3).[21] This makes it unlikely that USMCA provisions are driving the post-2021 surge in rerouting.

Second, one might worry that trade policy uncertainty surrounding the USMCA delayed rerouting. This explanation is also difficult to reconcile with the data. If uncertainty were the dominant friction, firms would be expected to postpone sunk investment. Instead, the warehousing evidence in Section 6.1 shows substantial investment in border logistics beginning soon after the tariff escalation. This is the opposite of what a *wait-and-see* mechanism would predict under high uncertainty (Dixit and Pindyck, 1994; Bloom, 2009). Consistent with this interpretation, contemporaneous assessments show that USMCA-related uncertainty eased after the October 2018 in-principle agreement (USITC Report, 2019; IMF, 2018, 2019).

[21]This is consistent with our model (Appendix Section B) in which rerouting occurs when the effective tariff wedge is sufficiently large relative to the fixed and variable costs of rerouting. This condition is more likely to hold for products with low MFN rates.

6.6 Tariff Thresholds for Rerouting

So far, we have shown that border logistics capacity governs the timing of adjustment. We now show that this timing is relevant only when the tariff wedge is sufficiently large to make rerouting viable. Specifically, the initial decision to reroute is fundamentally dependent on a large tariff wedge that justifies navigating rerouting frictions. Our model in Appendix Section B predicts that small tariff increases provide insufficient incentives for rerouting due to the presence of pecuniary and nonpecuniary costs. For low tariffs, the relevant prediction is not a delayed adjustment, but a complete absence of adjustment, i.e., no rerouting.

To test this prediction, we estimate Equation 1 for products targeted in the 2019 tranche of tariffs, which faced a significantly lower effective tariff increase of 7.5 percentage points compared to the 25 percent tariff for products targeted in 2018-Q3. Figure 10 shows no evidence of rerouting for these products targeted in 2019, with insignificant post-tariff coefficients.[22] These results indicate that the effective tariff rate that triggers rerouting falls is above 7.5 percent, but below 25 percent based on our baseline estimates.

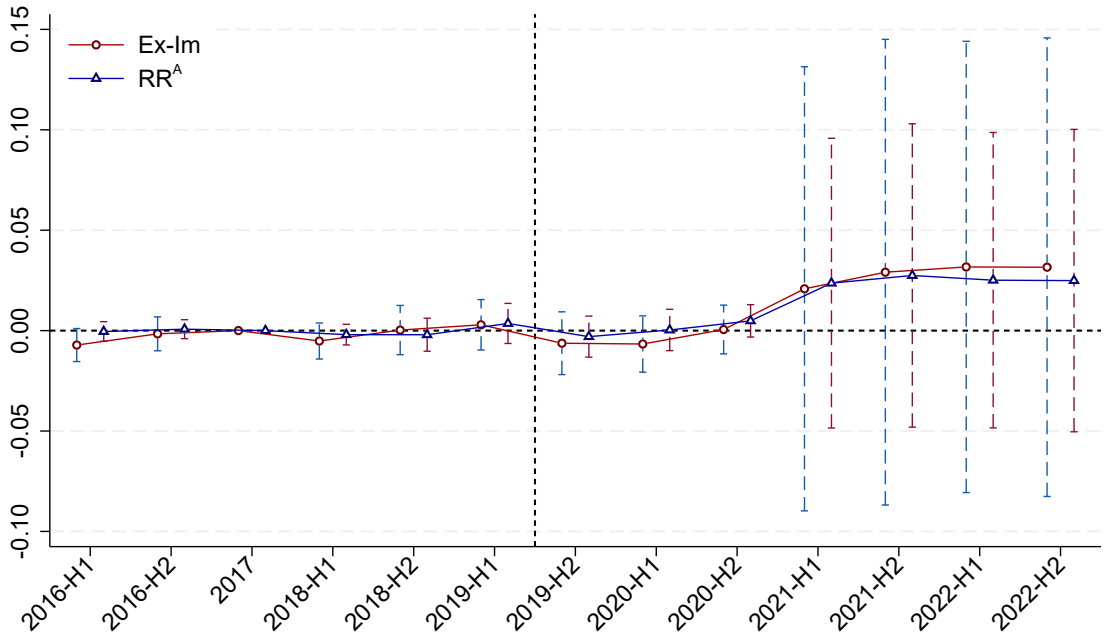
In summary, these findings are consistent with the model's prediction that only sufficiently large tariff shocks trigger costly adjustments such as rerouting through Mexico; and conditional on such incentives, logistics capacity constraints dictate the dynamics of rerouting.

7 Quantification: Rerouting and Fiscal Leakage

In this section, we quantify the aggregate value of trade rerouting and the associated fiscal leakage from regulatory arbitrage. We rely on the event study estimates from Equation 1 and post-shock aggregate trade volumes to recover the dollar value of circumvention. A key implication of our mechanism is that fiscal leakage is negligible in the short run, when rerouting does not materialize, and economically meaningful once logistical capacity constraints relax.

[22] In this specification, the treatment group comprises products targeted in 2019, while the control group consists of products never subject to US tariffs during this entire period. We exclude products targeted in the 2018 tranche from the estimation sample.

Figure 10: Tariff Magnitude and Rerouting: 2019 Tariff Evidence



Notes: This figure reports event-study estimates of rerouting for products targeted by US tariffs on Chinese imports implemented in 2019-H2. The figure reports estimates for two measures of rerouting, $Ex{-}Im$ and RR^A. Regressions are at the firm × product (HS 8-digit) × quarter level. All regressions include HS-4 × Quarter-Year and Firm × HS 8-digit fixed effects. Coefficients are reported relative to the baseline year 2017. Standard errors are clustered at the HS 8-digit level, and 95 percent confidence intervals are shown.

Table 5 presents the results. Columns (1)–(2) report results using our baseline value-adjusted measure ($\theta = 0.2$) separately for 2019–2020 (short-run) and 2021–2022 (medium-run). To obtain the aggregate rerouting value, we sum the observed rerouted value of tariffed products for which the adjusted measure RR^A is nonzero in a given period and scale this base by the treatment-induced percentage increase implied by the corresponding DiD estimates. This yields an aggregate rerouting flow of USD 300 million per year in 2021–2022, while the implied rerouting flow in 2019–2020 is close to zero. Given that products in our sample face a 25 percent tariff, the medium-term rerouting flow corresponds to an annual tariff revenue loss of USD 75 million for the US Treasury. Consistent with the event-study dynamics, the implied short-term fiscal leakage is negligible.

To benchmark the magnitude of the medium-term rerouting surge, we compare it to the broader increase in Mexican imports of tariffed products from China. The value of imports in these tariffed product lines increased by USD 6.2 billion annually between 2016–2017 and 2021–2022, so our baseline rerouting estimate accounts for 4.8 percent of this aggregate import surge. As a second benchmark, rerouted flows equal roughly 13.6 percent of USD 2.2 billion pre-period imports of tariffed products into Mexico.

We note that the estimate in column (2) is a lower bound for total rerouting activity because it focuses on intrafirm, same-product rerouting and imposes a conservative 20 percent domestic value-added threshold. Columns (3)–(4) report medium-term sensitivity and diagnostics. Relaxing the domestic value-added threshold to $\theta = 0.5$ raises the estimated rerouted value to USD 335 million (column (3)). For transparency, column (4) presents the estimates using unadjusted measure, which yields a significantly larger estimate of USD 1.6 billion in rerouting. This higher value reflects both a larger DiD coefficient and misclassification of high value-added cases as rerouting leading to a greater increase in the value of rerouting. The divergence highlights the critical importance of accounting for value addition; ignoring this factor leads to overestimation of rerouting by a factor of five.

Finally, because the medium-term estimate is an annual flow, the implied fiscal cost

Table 5: Quantification: Aggregate Rerouting and Fiscal Leakage Estimates

	Short-run	Medium-run		
	$\theta = 0.2$	$\theta = 0.2$	$\theta = 0.5$	RR^U
	(1)	(2)	(3)	(4)
Panel A: Parameter Estimates				
DiD Coefficient	0.00	0.05	0.06	0.06
Panel B: Aggregate Implications				
Δ Rerouted Value *(USD Million per year)*	5	300	365	1593
Implied Tariff Revenue Loss *(USD Million per year)*	1	75	91	398
Share of Import Surge *(% of Δ Mexican Imports)*	0.036	4.81	5.86	25.57

Notes: This table quantifies the aggregate value of trade rerouting based on the difference-in-differences estimates. The DiD coefficient is the mean of the coefficient values based on Equation 1. We use the coefficients from 2019-2020 (short-run) for column (1), and coefficient values from 2021-2022 (medium-run) for the other three columns. For columns (1)–(3), the outcome measure is the value-adjusted rerouting indicator RR^A with $\theta = 0.2$ in columns (1) and (2) and $\theta = 0.5$ in column (3). The outcome measure in column (4) is the unadjusted rerouting measure. Δ Rerouted Value is calculated by applying the implied percentage increase (the DiD coefficient relative to the pre-period mean) to the average annual rerouted value observed in the corresponding post-shock period. To calculate these base values, we utilize the value-adjusted RR^A measure for columns (1)–(3) and the unadjusted RR^U measure for column (4). This represents the component of rerouted trade attributable to the tariff-induced adjustment. Implied Tariff Revenue Loss corresponds to the statutory tariff rate of 25 percent on the products tariffed in Q3-2018. Share of Import Surge compares the rerouted value to the average increase of USD 6.2 billion in Mexican imports from China in tariffed products between 2021–2022 vs. 2016–2017.

accumulates over time: At USD 75 million per year, holding tariff policy and enforcement constant, a ten-year horizon amounts to USD 0.75 billion in lost tariff revenue.

8 Conclusion

Our paper provides a new channel for delayed trade adjustment. We show that the speed of trade reallocation after tariff changes is governed by the elasticity of logistics corridors. Using the 2018 US–China trade war as a laboratory and utilizing multiple independent data sources, we show that while the episode created strong incentives for regulatory arbitrage through Mexico, the trade response was initially constrained by a shortage of essential border infrastructure. We document a binding physical floor in border warehousing markets, where

vacancy reached stock-out conditions and prevented an immediate scaling of rerouted trade. The multiyear delay in adjustment was not primarily a failure of firm-level preparation, but rather a reflection of infrastructure gestation lags—the time required to plan, permit, and deliver industrial capacity needed to support new trade flows. Our findings therefore provide a corridor-based microfoundation for the divergence between short- and long-term trade elasticities. Unlike internal adjustment costs for firms, this channel operates outside their span of control and is specific to physical capacity of trade corridors.

The logistics capacity frictions we document also differ from transportation bottlenecks emphasized in prior trade research. Mobile inputs such as trucks, ships, or container slots can be reallocated and rationed through prices. By contrast, locally fixed and contractually rigid infrastructure, such as cross-docking and warehousing near ports of entry, cannot be scaled quickly in response to demand. As a result, trade reallocation can remain muted until new capacity is delivered. This implies that countries may be unable to benefit immediately from large trade shocks when corridor capacity is constrained. Although our analysis focuses on a land-based trade corridor, similar adjustment frictions may arise in other settings when trade reallocation depends on localized logistics infrastructure whose capacity is constrained in the short-run.

More broadly, our paper speaks to the efficiency costs of trade reallocation through capacity-constrained logistics nodes. In our setting, shifting supply chains requires additional logistics, including extra trucking legs, cross-docking, and administrative processing, that are real resource costs generated by the corridor bottleneck and can contribute to welfare losses. This implies that the welfare costs of the trade war include not only higher consumer prices (Fajgelbaum et al., 2020; Amiti et al., 2019) but also the resource diversion required to execute reallocation through congested corridor infrastructure. As global supply chains increasingly shift toward multi-leg regional hubs to navigate geopolitical tensions, our findings underscore that the physical pipe, rather than the tariff wedge, may become the binding constraint on the speed and level of trade reallocation.

References

Aggarwal, S. and I. Chatterjee (2025): "A Road for all Seasons: Market Access and Inter-temporal Arbitrage in Rural India," .

Alfaro, L. and D. Chor (2023): "Global supply chains: The looming "great reallocation"," Tech. rep., National Bureau of Economic Research.

Allen, T. and C. Arkolakis (2022): "The welfare effects of transportation infrastructure improvements," *The Review of Economic Studies*, 89, 2911–2957.

Allen, T. and D. Atkin (2022): "Volatility and the Gains from Trade," *Econometrica*, 90, 2053–2092.

Alvarez, R., H. Faruq, and R. A. López (2013): "Is previous export experience important for new exports?" *The Journal of Development Studies*, 49, 426–441.

Amiti, M., S. J. Redding, and D. E. Weinstein (2019): "The impact of the 2018 tariffs on prices and welfare," *Journal of Economic perspectives*, 33, 187–210.

Antras, P. and A. Costinot (2011): "Intermediated Trade," *The Quarterly Journal of Economics*, 126, 1319–1374.

Antràs, P. and S. R. Yeaple (2014): "Multinational firms and the structure of international trade," *Handbook of international economics*, 4, 55–130.

Arvis, J.-F., R. C. Carruthers, G. M. Smith, and C. Willoughby (2011): *Connecting Landlocked Developing Countries to Markets: Trade Corridors in the 21st Century*, Directions in Development: Trade, Washington, DC: The World Bank.

Bhagwati, J. N. and T. N. Srinivasan (1980): "Revenue Seeking: A Generalization of the Theory of Tariffs," *Journal of Political Economy*, 88, 1069–1087.

Blonigen, B. A. (2002): "Tariff-jumping antidumping duties," *Journal of international Economics*, 57, 31–49.

Bloom, N. (2009): "The Impact of Uncertainty Shocks," *Econometrica*, 77, 623–685.

Boehm, C. E., A. A. Levchenko, and N. Pandalai-Nayar (2023): "The long and short (run) of trade elasticities," *American Economic Review*, 113, 861–905.

Bown, C. P. (2021): "The US–China trade war and Phase One agreement," *Journal of Policy Modeling*, 43, 805–843.

Brancaccio, G., M. Kalouptsidi, and T. Papageorgiou (2020): "Geography, transportation, and endogenous trade costs," *Econometrica*, 88, 657–691.

——— (2024): "Investment in infrastructure and trade: The case of ports," Tech. rep., National Bureau of Economic Research.

Brueckner, J. K. and S. S. Rosenthal (2025): "Tenant riskiness, contract length, and the term structure of commercial leases," *Management Science*.

Bruno, V. and H. S. Shin (2023): "Dollar and exports," *The review of financial studies*, 36, 2963–2996.

Burfisher, M. E., F. Lambert, and M. T. D. Matheson (2019): *NAFTA to USMCA: What is Gained?*, International Monetary Fund.

Cavallo, A., G. Gopinath, B. Neiman, and J. Tang (2021): "Tariff pass-through at the border and at the store: Evidence from us trade policy," *American Economic Review: Insights*, 3, 19–34.

Chakrabarti, A. S., K. Mahajan, and S. Tomar (2025): "Trade disruptions and reshoring," *American Economic Journal: Applied Economics*, 17, 239–270.

Chaney, T. (2014): "The network structure of international trade," *American economic review*, 104, 3600–3634.

Chang, P.-L., K. Yao, and F. Zheng (2021): "The response of the Chinese economy to the US-China Trade War: 2018-2019," .

Colantone, I., G. Ottaviano, and P. Stanig (2022): "The backlash of globalization," in *Handbook of international economics*, Elsevier, vol. 5, 405–477.

Conconi, P., M. García-Santana, L. Puccio, and R. Venturini (2018): "From final goods to inputs: the protectionist effect of rules of origin," *American Economic Review*, 108, 2335–2365.

Coşar, A. K. and P. D. Fajgelbaum (2016): "Internal geography, international trade, and regional specialization," *American Economic Journal: Microeconomics*, 8, 24–56.

Dang, A. H., K. Krishna, and Y. Zhao (2023): "Winners and losers from the US-China trade war," Tech. rep., National Bureau of Economic Research.

De Wulf, L. and J. B. Sokol (2005): *Customs modernization handbook*, World Bank Publications.

Dixit, A. K. and R. S. Pindyck (1994): *Investment under Uncertainty*, Princeton, NJ: Princeton University Press.

Donaldson, D. (2018): "Railroads of the Raj: Estimating the impact of transportation infrastructure," *American Economic Review*, 108, 899–934.

Donaldson, D. and R. Hornbeck (2016): "Railroads and American economic growth: A âmarket accessâ approach," *The Quarterly Journal of Economics*, 131, 799–858.

Drozd, L. A., S. Kolbin, and J. B. Nosal (2021): "The trade-comovement puzzle," *American Economic Journal: Macroeconomics*, 13, 78–120.

Ducruet, C., R. Juhász, D. K. Nagy, and C. Steinwender (2024): "All aboard: The effects of port development," *Journal of International Economics*, 151, 103963.

Dutt, A., G. Panayotov, D. Roy, and X. Wen (2025): "Is a Lack of Information Limiting Sanctions Enforcement?" Working Paper.

Fajgelbaum, P., P. Goldberg, P. Kennedy, A. Khandelwal, and D. Taglioni (2024): "The US-China trade war and global reallocations," *American Economic Review: Insights*, 6, 295–312.

Fajgelbaum, P. D., P. K. Goldberg, P. J. Kennedy, and A. K. Khandelwal (2020): "The return to protectionism," *The quarterly journal of economics*, 135, 1–55.

Fajgelbaum, P. D. and E. Schaal (2020): "Optimal transport networks in spatial equilibrium," *Econometrica*, 88, 1411–1452.

Feenstra, R. C. and G. H. Hanson (2004): "Intermediaries in entrepot trade: Hong Kong re-exports of Chinese goods," *Journal of Economics & Management Strategy*, 13, 3–35.

Flaaen, A., F. Haberkorn, L. Lewis, A. Monken, J. Pierce, R. Rhodes, and M. Yi (2023): "Bill of lading data in international trade research with an application to the COVID-19 pandemic," *Review of International Economics*, 31, 1146–1172.

Flaaen, A., A. Hortaçsu, and F. Tintelnot (2020): "The production relocation and price effects of US trade policy: the case of washing machines," *American Economic Review*, 110, 2103–2127.

Fontagné, L., H. Guimbard, and G. Orefice (2022): "Tariff-based product-level trade elasticities," *Journal of International Economics*, 137, 103593.

Freund, C. (2025): "The China Wash: Tracking Products To Identify Tariff Evasion Through Transshipment," Policy report, UC San Diego School of Global Policy and

Strategy, 21st Century China Center and Center for Commerce and Diplomacy, La Jolla, CA.

Frittelli, J. (2014): "Status of Mexican trucks in the United States: Frequently asked questions," .

Ganapati, S., W. F. Wong, and O. Ziv (2024): "Entrepot: Hubs, scale, and trade costs," *American Economic Journal: Macroeconomics*, 16, 239–278.

Glancy, D., R. Kurtzman, and L. Loewenstein (2026): "JUE Insight: Shovel ready projects and commercial construction activityâs long and variable lags," *Journal of Urban Economics*, 151, 103816.

Grossman, G. M., E. Helpman, and S. J. Redding (2024): "When tariffs disrupt global supply chains," *American Economic Review*, 114, 988–1029.

Gupta, A., V. Mittal, and S. Van Nieuwerburgh (2022): "Work from home and the office real estate apocalypse," .

Hanson, G. H. (1996): "Localization Economies, Vertical Organization, and Trade," *American Economic Review*, 86, 1266–1278.

IMF (2018): "Mexico: 2018 Article IV Consultation—Press Release; Staff Report; and Staff Statement," IMF Country Report 18/307, International Monetary Fund, iMF Country Report No. 18/307.

——— (2019): "Canada: 2019 Article IV Consultation—Press Release; and Staff Report," IMF Country Report 19/175, International Monetary Fund, iMF Country Report No. 19/175.

Irwin, D. A. (2020): "The pandemic adds momentum to the deglobalization trend," *Peterson Institute for International Economics*, 23.

Iyoha, E., E. Malesky, J. Wen, and S.-J. Wu (2025): "Exports in disguise? Trade rerouting during the US–China trade war," .

Jakubik, A. and M. Ruta (2023): "Trading with friends in uncertain times," *Journal of Policy Modeling*, 45, 768–780.

Lanteri, A. and A. A. Rampini (2023): "Constrained-Efficient Capital Reallocation," *American Economic Review*, 113, 354â95.

Lee, J. and K. K. Rhee (2025): "The impact of the US-China trade war on Vietnam's US Exports," *Available at SSRN 5252880*.

Liu, X. and H. Shi (2019): "Anti-dumping duty circumvention through trade rerouting: Evidence from Chinese exporters," *The World Economy*, 42, 1427–1466.

Ma, H., J. Ning, and M. J. Xu (2021): "An eye for an eye? The trade and price effects of China's retaliatory tariffs on US exports," *China Economic Review*, 69, 101685.

Madsen, E., M. Rotemberg, S. Traiberman, and S. Wang (2025): "Tariffs and State Capacity: A Specific Example," Tech. rep., National Bureau of Economic Research.

Millar, J. N., S. D. Oliner, and D. E. Sichel (2016): "Time-to-plan lags for commercial construction projects," *Regional Science and Urban Economics*, 59, 75–89.

Nguyen, A. and S. Lim (2023): "Structural transformation in the era of trade protectionism," *Available at SSRN 4426955*.

Rauch, J. E. (1999): "Networks versus markets in international trade," *Journal of international Economics*, 48, 7–35.

Rotunno, L., S. Roy, A. Sakakibara, and P.-L. Vezina (2023): "Trade policy and jobs in Vietnam: The unintended consequences of Trumpâs trade war," Tech. rep., Center for Open Science.

Rotunno, L., P.-L. Vézina, and Z. Wang (2013): "The rise and fall of (Chinese) African apparel exports," *Journal of development Economics*, 105, 152–163.

Ruhl, K. J. et al. (2008): "The international elasticity puzzle," .

Schafhäutle, S. G. and G. S. Sran (2024): "Redacted Identities in Shipment Records: Evidence from Forced Labor Scrutiny in Supply Chains," *Available at SSRN 5140247*.

Trew, A. (2020): "Endogenous infrastructure development and spatial takeoff in the first industrial revolution," *American Economic Journal: Macroeconomics*, 12, 44–93.

USITC Report (2019): "U.S.-Mexico-Canada Trade Agreement: Likely Impact on the U.S. Economy and on Specific Industry Sectors (with Errata)," Report Publication 4889, United States International Trade Commission, investigation No. TPA-105-003.

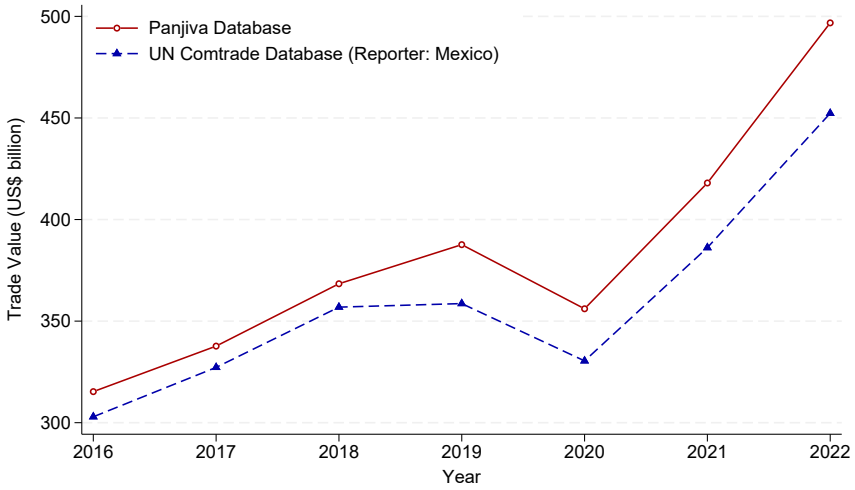
Utar, H., A. C. Zurita, and L. Torres (2025): "The US-China trade war and the relocation of global value chains to Mexico," *Review of Economics and Statistics*, 1–47.

Waugh, M. E. (2019): "The consumption response to trade shocks: Evidence from the US-China trade war," Tech. rep., National Bureau of Economic Research.

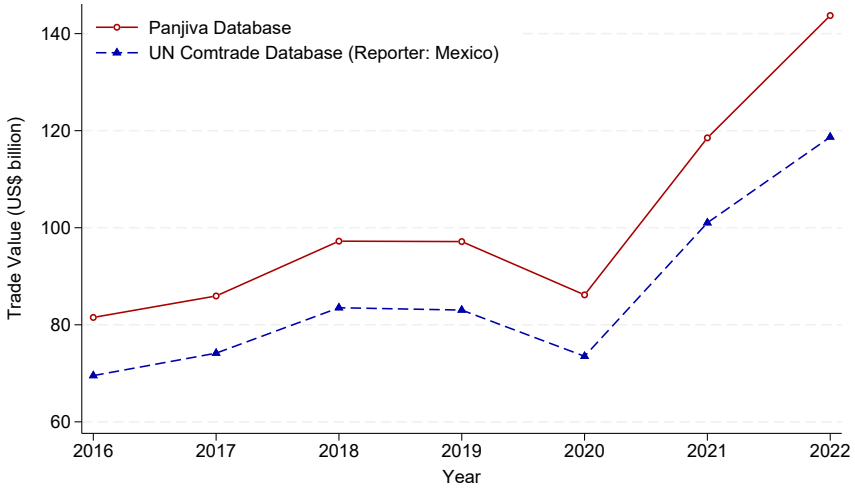
Wu, S.-J. (2024): "Foreign Profit Shifting and The Welfare Responses to The US–China Trade War: Evidence from Manufacturers in Vietnam (Job Market Paper)," Tech. rep., Technical report.

A Appendix: Tables and Figures

Figure A.1: Validation of Panjiva Data against UN Comtrade



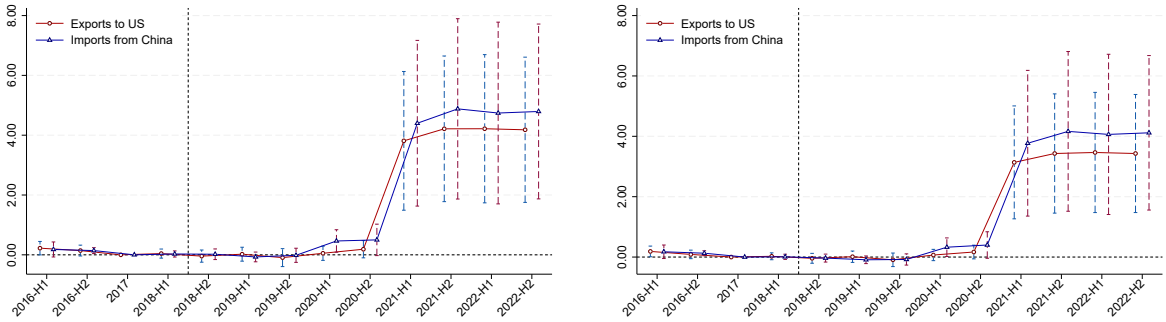
(a) Mexico's Exports to the US



(b) Mexico's Imports from China

Notes: This figure compares annual aggregate trade flows in the Panjiva shipment-level data with the corresponding official UN Comtrade totals over the 2016–2022 period. Panel (a) reports Mexico's exports to the United States, and Panel (b) reports Mexico's imports from China. Trade values are expressed in billions of US dollars.

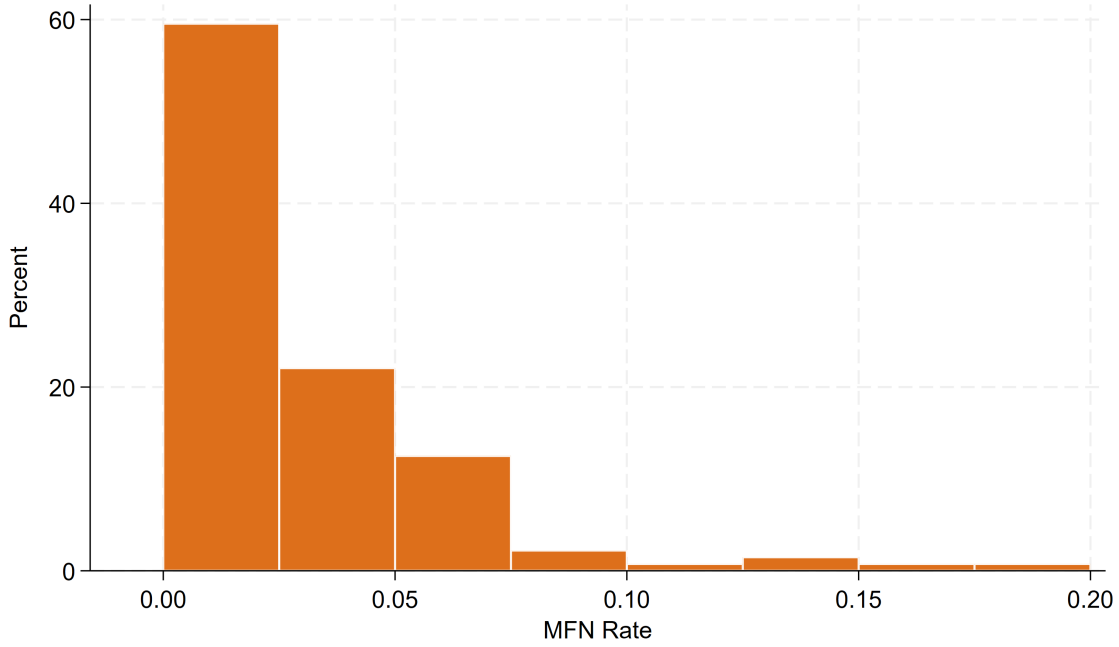
Figure A.2: Impact of US Tariffs on Mexican Firms' Trade with the US and China



(a) Trade Value (b) Trade Quantity

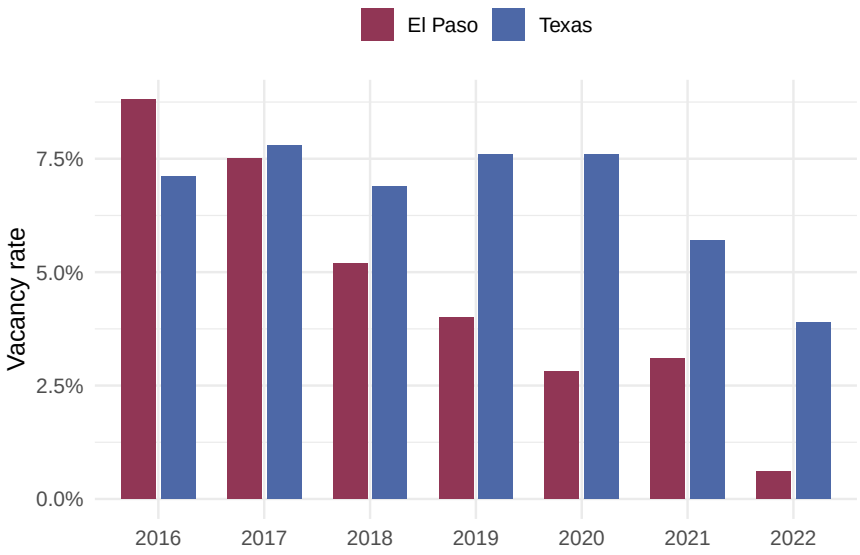
Notes: This figure reports event-study estimates of the effects of US tariffs on Mexican firms' exports to the US and imports from China. Panel (a) uses trade value, and Panel (b) uses trade quantity. The dependent variable is transformed as $\log(0.01 + y)$, where y denotes the underlying trade outcome. Results are similar with ppml estimation (available on request). Regressions are at the firm × product (HS 8-digit) × quarter level. All regressions include HS-4 × QnY and Firm × HS 8-digit fixed effects. Standard errors are clustered at the HS 8-digit level, and 95 percent confidence intervals are shown.

Figure A.3: Distribution of US MFN Tariff Rates for Rerouted Products

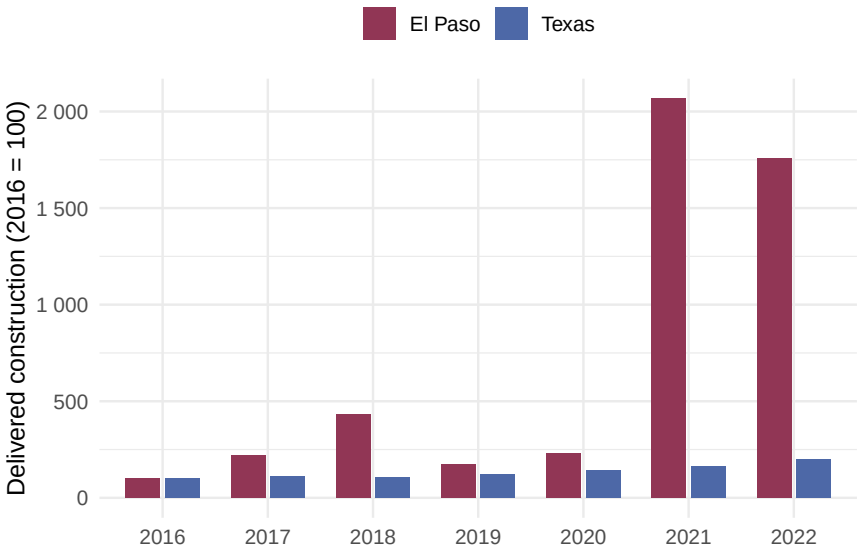


Notes: This figure plots the distribution of US most favored nation (MFN) ad valorem tariff rates for the set of products identified as rerouted via Mexico in the data, i.e., $Ex - Im = 1$. The sample consists of 136 HS 8-digit products for which the rerouting indicator equals one in the post-2018Q2 period. MFN tariff rates are the statutory duties that apply to imports entering the United States outside the preferential terms of a free trade agreement. Data source: United States International Trade Commission.

Figure A.4: Industrial Vacancy and Delivered Construction: El Paso vs. Texas Average



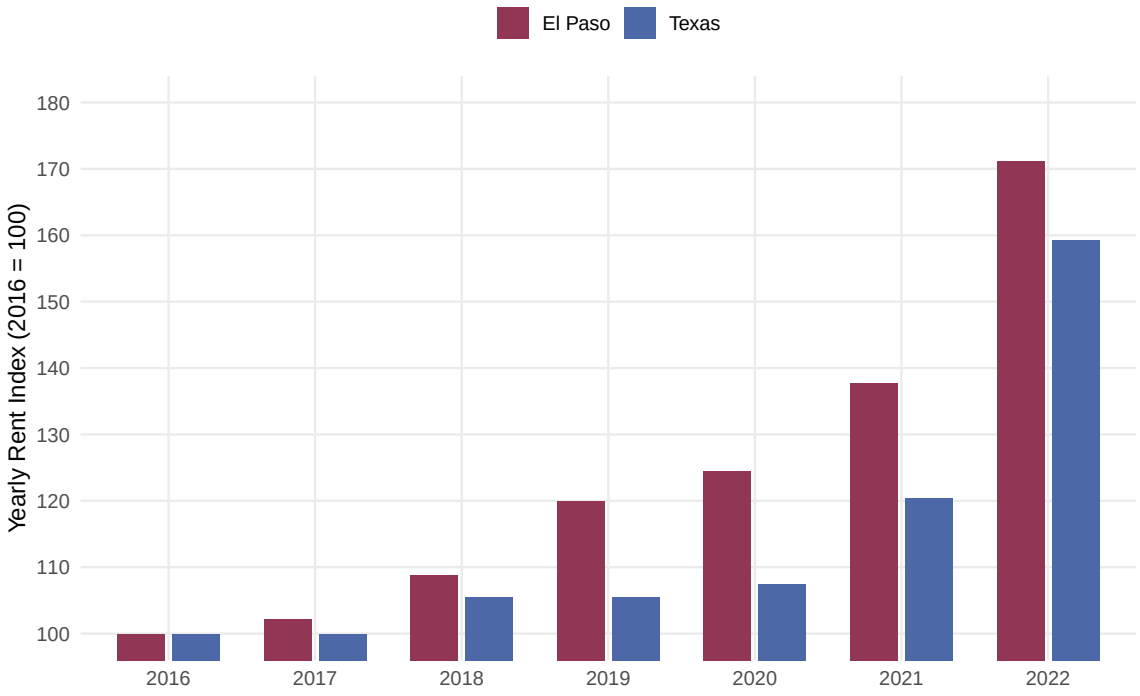
(a) Vacancy Rate



(b) Delivered Construction Index

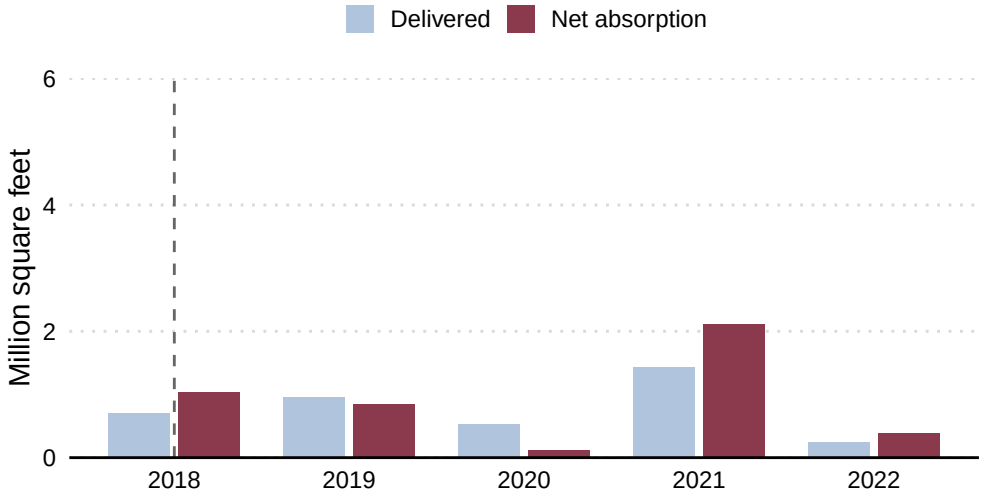
Notes: Panel (a) reports annual industrial vacancy rates, measured as the share of industrial warehousing inventory that is vacant, for El Paso and for the average across the major Texas markets in the sample. Panel (b) reports an index of annual delivered industrial construction for the same markets, normalized to 100 in 2016 separately for El Paso and the Texas average. Texas numbers are based on the average across Dallas, Houston, Austin, San Antonio, and El Paso. Source: CBRE Industrial MarketView Reports, hand-collected and compiled by the authors.

Figure A.5: Industrial Asking Rent: El Paso vs. Texas Average

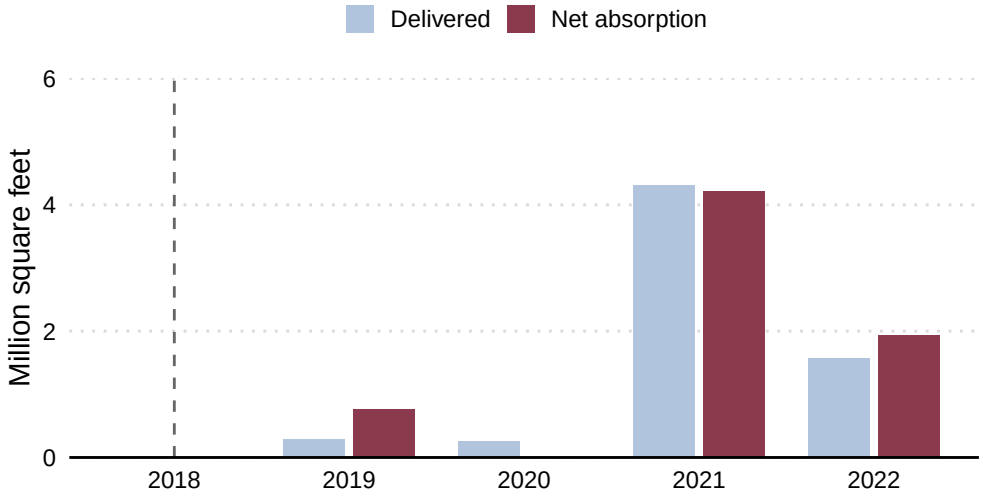


Notes: This figure reports the annual industrial asking rent index for El Paso and for the average across the major Texas markets in the sample. Texas numbers are based on the average across Dallas, Houston, Austin, San Antonio, and El Paso. Source: CBRE Industrial MarketView Reports, hand-collected and compiled by the authors.

Figure A.6: Robustness: Industrial Real Estate Dynamics in Other US–Mexico Border Cities



(a) Laredo



(b) Otay Mesa

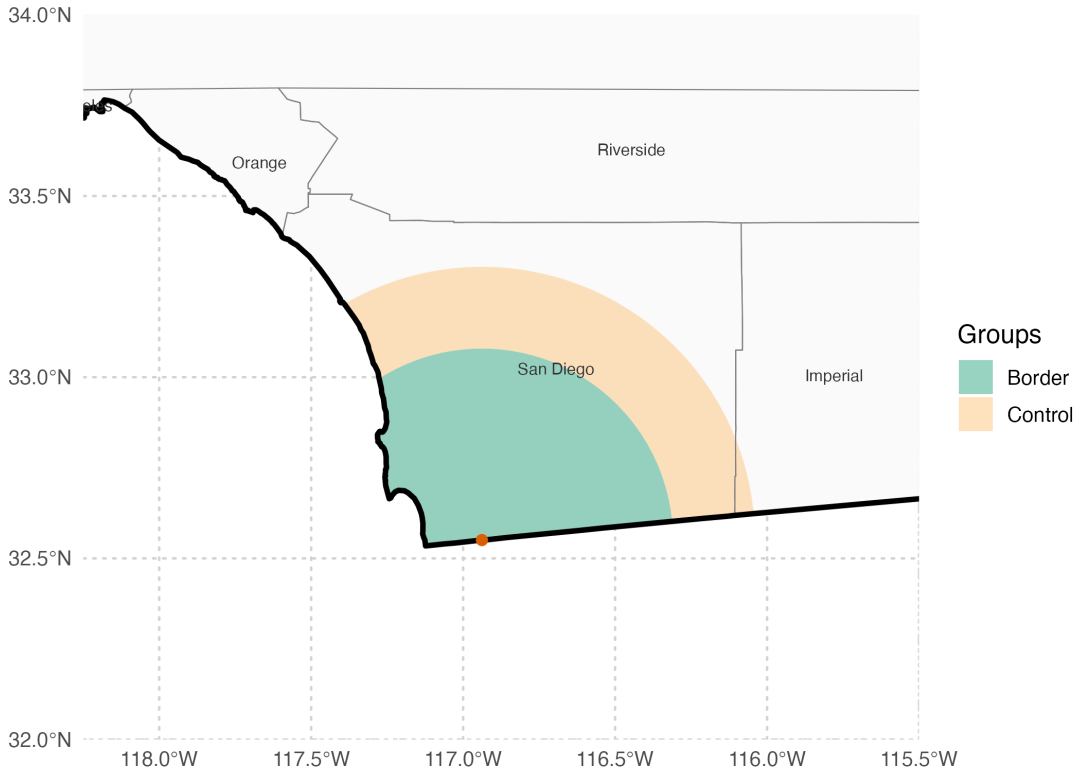
Notes: This figure reports industrial real estate dynamics in two other US–Mexico border cities. Panel (a) reports industrial real estate dynamics for Laredo, and Panel (b) reports the same for Otay Mesa. The bars represent annual totals for delivered construction (supply) and net absorption (realized demand), measured in millions of square feet. The vertical dashed line denotes 2018, marking the onset of the US–China trade war. Data are available for 2018–2022 in Laredo and for 2019–2022 in Otay Mesa. Source: CBRE Industrial MarketView Reports, hand-collected and compiled by the authors.

Figure A.7: Warehouse Activity near the Ysleta Port of Entry



Notes: This photograph shows containers and trucks at a warehouse facility near the Ysleta Port of Entry in El Paso, Texas, during the post-trade war period. Source: Google Maps imagery.

Figure A.8: Illustration: Construction of Border and Control Bands



Notes: This figure illustrates the construction of the border and control bands around Otay Mesa in the San Diego area. The shaded areas correspond to the 0–70 km border band and the 70–100 km control band. The orange dot marks the Otay Mesa Port of Entry. The solid black line denotes the US–Mexico border.

Table A.1: Transport Modes for Mexico–US Exports

	Transactions		Value	
	2016–2017	2021–2022	2016–2017	2021–2022
	(1)	(2)	(3)	(4)
Truck	90.89	91.30	72.85	72.36
Rail	1.56	1.40	16.01	12.64
Sea	0.82	0.76	7.01	9.83
Air	6.13	6.11	3.32	4.17
Pipeline	0.00	0.00	0.05	0.02
Others	0.60	0.43	0.76	0.98

Notes: This table reports the share of Mexico–US export transactions accounted for by each transport mode. The first two columns report shares by transaction count, and the last two columns report shares by export value. All shares are expressed as percentages of the annual total.

Table A.2: Top Tariffed Products Imported from China into Mexico

HS-4 Digit	Description	Total Value (USD Million)
8529	Parts suitable for use solely or principally with the apparatus of headings 8524 to 8528	3,287
8703	Motor cars and other motor vehicles principally designed for the transport of persons (other than those of heading 8702), including station wagons and racing cars:	2,229
8414	Air or vacuum pumps, air or other gas compressors and fans; ventilating or recycling hoods incorporating a fan, whether or not fitted with filters; gas-tight biological safety cabinets, whether or not fitted with filters; parts thereof:	749
8409	Parts suitable for use solely or principally with the engines of heading 8407 or 8408:	407
4011	New pneumatic tires, of rubber:	363
8543	Electrical machines and apparatus, having individual functions, not specified or included elsewhere in this chapter; parts thereof:	336
8708	Parts and accessories of the motor vehicles of headings 8701 to 8705:	323
8471	Automatic data processing machines and units thereof; magnetic or optical readers, machines for transcribing data onto data media in coded form and machines for processing such data, not elsewhere specified or included:	297
4202	Trunks, suitcases, vanity cases, attache cases, briefcases, school satchels, spectacle cases, binocular cases, camera cases, musical instrument cases, gun cases, holsters and similar containers; traveling bags, insulated food or beverage bags, toiletry bags, knapsacks and backpacks, handbags, shopping bags, wallets, purses, map cases, cigarette cases, tobacco pouches, tool bags, sports bags, bottle cases, jewelry boxes, powder cases, cutlery cases and similar containers, of leather or of composition leather, of sheeting of plastics, of textile materials, of vulcanized fiber or of paperboard, or wholly or mainly covered with such materials or with paper:	176
6505	Hats and other headgear, knitted or crocheted, or made up from lace, felt or other textile fabric, in the piece (but not in strips), whether or not lined or trimmed; hair-nets of any material, whether or not lined or trimmed:	78

Notes: This table reports the top 10 HS 4-digit product categories with the highest average annual import value from China into Mexico over 2021–2022 among products targeted by the US Section 301 tariffs imposed in 2018-Q3. Data source: S&P Panjiva.

Table A.3: Rerouting of Trade via Mexico: Difference-in-Differences Estimates

Dep. Var	Ex-Im	Ex-Im$_{1Y}$	RR^A	RR^S
	(1)	(2)	(3)	(4)
Treat × Post	0.037**	0.043**	0.022**	0.021**
	(0.014)	(0.015)	(0.008)	(0.008)
Observations	6402256	6402256	6402256	6402256
R-Squared	0.499	0.540	0.434	0.436
Mean	0.11	0.13	0.07	0.07
HS-4 × QnY FE	✓	✓	✓	✓
Firm × HS-8 FE	✓	✓	✓	✓

Notes: The dependent variable in columns (1) and (2) is an extensive-margin rerouting indicator. In column (1), the indicator equals one if a firm imports an HS 8-digit product from China and exports the same HS 8-digit product to the US in the same quarter. In column (2), the indicator is defined analogously, except that imports may occur either in the current quarter or in any of the previous three quarters. The dependent variables in columns (3) and (4) are the adjusted (RR^A) and smoothed (RR^S) rerouting measures. *Post* is a binary indicator that equals 1 after 2018-Q2, else zero. $Treat$ is a binary indicator that equals 1 for products targeted by the 2018 US Section 301 tariffs, else zero. Regressions are at the firm × product (HS 8-digit) × quarter level. Standard errors, clustered at the HS 8-digit level, are in parentheses. ** p < 0.01, * p < 0.05, ^+p<0.1.

Table A.4: Accounting for "Case B" Rerouting

Dep. Var	Ex-Im^{Any}	Ex-Im$_{1Y}^{Any}$
	(1)	(2)
Treat × Post	0.046**	0.046**
	(0.016)	(0.016)
Observations	6402256	6402256
R-Squared	0.594	0.595
Mean	0.16	0.16
HS-4 × QnY FE	✓	✓
Firm × HS-8 FE	✓	✓

Notes: The dependent variable in both columns is an extensive-margin indicator for "Case B" rerouting. In column (1), the indicator equals one if a firm imports any HS 8-digit product from China and exports the tariffed HS 8-digit product to the US in the same quarter. In column (2), the indicator is defined analogously, except that imports may occur either in the current quarter or in any of the previous three quarters. *Post* is a binary indicator that equals 1 after 2018-Q2, else zero. $Treat$ is a binary indicator that equals 1 for products targeted by the 2018 US Section 301 tariffs, else zero. Regressions are at the firm × product (HS 8-digit) × quarter level. Standard errors, clustered at the HS 8-digit level, are in parentheses. ** p < 0.01, * p < 0.05, ^+p<0.1.

Table A.5: Robustness: Rerouting Estimates Using the Unadjusted Measure

Dep. Var	Value	Quantity
	(1)	(2)
Treat × Post	0.026**	0.028*
	(0.010)	(0.011)
Observations	6402256	6402256
R-Squared	0.465	0.475
HS-4 × QnY FE	✓	✓
Firm × HS-8 FE	✓	✓

Notes: The dependent variable is the unadjusted rerouting measure, value-based in column (1) and quantity-based in column (2). *Post* is a binary indicator that equals 1 after 2018-Q2, else zero. *Treat* is a binary indicator that equals 1 for products targeted by the 2018 US Section 301 tariffs, else zero. Regressions are at the firm × product (HS 8-digit) × quarter level. Standard errors, clustered at the HS 8-digit level, are in parentheses. ** p < 0.01, * p < 0.05, ^{+}p<0.1.

Table A.6: Rerouting of Trade via Mexico: Quantity Measure

Dep. Var	Quantity	
	RR^A	RR^S
Treat ×	(1)	(2)
2016-H1	0.001	0.001
	(0.004)	(0.004)
2016-H2	0.007$^+$	0.006
	(0.004)	(0.004)
2018-H1	0.005	0.005
	(0.004)	(0.004)
2018-H2	0.001	0.001
	(0.003)	(0.004)
2019-H1	0.003	0.004
	(0.003)	(0.004)
2019-H2	–0.001	–0.001
	(0.003)	(0.004)
2020-H1	0.005	0.001
	(0.004)	(0.005)
2020-H2	0.005	0.005
	(0.004)	(0.004)
2021-H1	0.051*	0.061*
	(0.020)	(0.026)
2021-H2	0.054**	0.069**
	(0.019)	(0.026)
2022-H1	0.053**	0.066*
	(0.020)	(0.026)
2022-H2	0.050*	0.067*
	(0.020)	(0.026)
Observations	6402256	6402256
R-Squared	0.437	0.475
HS-4 × QnY FE	✓	✓
Firm × HS-8 FE	✓	✓

Notes: The dependent variable is the quantity-based rerouting measure defined in Equation 5. Column (1) is based on the adjusted measure, RR^A, and column (2) is based on the smoothed measure, RR^S. $Treat$ is a binary indicator that equals 1 for products targeted by the 2018 US Section 301 tariffs, else zero. The year 2017 serves as the baseline period. Regressions are at the firm × product (HS 8-digit) × quarter level. Standard errors, clustered at the HS 8-digit level, are in parentheses. ** p < 0.01, * p < 0.05, ^+p<0.1.

Table A.7: Rerouting: The Role of Product Differentiation and Elasticity

Dep. Var	Re-Routed			
	Ex-Im		RR^A	
	(1)	(2)	(3)	(4)
Treat × Post	–0.005	0.083*	–0.012	0.048*
	(0.015)	(0.035)	(0.016)	(0.021)
Treat × Post × Differentiated	0.044*		0.035$^+$	
	(0.021)		(0.019)	
Treat × Post × Elasticity		–0.006		–0.003
		(0.004)		(0.002)
Observations	6383720	6225576	6383720	6225576
R-Squared	0.499	0.498	0.434	0.433
Pr(F)	0.03	0.02	0.02	0.02
HS-4 × QnY FE	✓	✓	✓	✓
Firm × HS-8 FE	✓	✓	✓	✓

Notes: Columns (1) and (2) use an extensive-margin rerouting indicator ($Ex{-}Im$) that equals one if a firm imports an HS 8-digit product from China and exports the same HS 8-digit product to the US in a given quarter. Columns (3) and (4) use the adjusted rerouting measure, RR^A. "Differentiated" is the product differentiation measure from Rauch (1999), mapped to the HS 4-digit level. "Elasticity" is the elasticity measure from Fontagné et al. (2022), mapped to the HS 6-digit level. *Post* is a binary indicator that equals 1 after 2018-Q2, else zero. *Treat* is a binary indicator that equals 1 for products targeted by the 2018 US Section 301 tariffs, else zero. Regressions are at the firm × product (HS 8-digit) × quarter level. Standard errors, clustered at the HS 8-digit level, are in parentheses. ** p < 0.01, * p < 0.05, ^+p<0.1.

Table A.8: Robustness: Using Tariff Change as the Explanatory Variable

Dep. Var	Ex-Im	RR^A	RR^S
	(1)	(2)	(3)
Δ Tariff × Post	0.211*	0.133*	0.126*
	(0.099)	(0.061)	(0.059)
Observations	6402256	6402256	6402256
R-Squared	0.499	0.434	0.436
HS-4 × QnY FE	✓	✓	✓
Firm × HS-8 FE	✓	✓	✓

Notes: Column (1) use an extensive-margin rerouting indicator ($Ex{-}Im$) that equals one if a firm imports an HS 8-digit product from China and exports the same HS 8-digit product to the US in a given quarter. Columns (2) and (3) use adjusted (RR^A) and smoothed (RR^S) measures of rerouting. *Post* is a binary indicator that equals 1 after 2018-Q2, else zero. Δ Tariff is the change in tariff for products targeted by the 2018 US Section 301 tariffs, else zero. Regressions are at the firm × product (HS 8-digit) × quarter level. Standard errors, clustered at the HS 8-digit level, are in parentheses. ** p < 0.01, * p < 0.05, ^+p<0.1.

Table A.9: Robustness: Rerouting Estimates under Alternative Values of θ

	$\theta = 0.3$		$\theta = 0.5$	
Dep. Var	RR^A	RR^S	RR^A	RR^S
	(1)	(2)	(3)	(4)
Treat × Post	0.023**	0.022**	0.023**	0.023**
	(0.008)	(0.008)	(0.009)	(0.009)
Observations	6402256	6402256	6402256	6402256
R-Squared	0.436	0.440	0.443	0.448
HS-4 × QnY FE	✓	✓	✓	✓
Firm × HS-8 FE	✓	✓	✓	✓

Notes: Columns (1) and (3) use the adjusted rerouting measure, RR^A, and columns (2) and (4) use the smoothed rerouting measure, RR^S. Across columns, the parameter θ is allowed to vary as indicated in the table. *Post* is a binary indicator that equals 1 after 2018-Q2, else zero. $Treat$ is a binary indicator that equals 1 for products targeted by the 2018 US Section 301 tariffs, else zero. Regressions are at the firm × product (HS 8-digit) × quarter level. Standard errors, clustered at the HS 8-digit level, are in parentheses. ** p < 0.01, * p < 0.05, ^{+}p<0.1.

Table A.10: Robustness: Exporters with the US as Their Main Export Destination

	US Exports Share ≥ 80%			US Exports Share ≥ 90%		
Dep. Var	Ex-Im	RR^A	RR^S	Ex-Im	RR^A	RR^S
	(1)	(2)	(3)	(4)	(5)	(6)
Treat × Post	0.029*	0.018**	0.017**	0.029*	0.018**	0.017**
	(0.013)	(0.007)	(0.006)	(0.012)	(0.006)	(0.006)
Observations	4975152	4975152	4975152	4670652	4670652	4670652
R-Squared	0.498	0.418	0.420	0.493	0.413	0.415
HS-4 × QnY FE	✓	✓	✓	✓	✓	✓
Firm × HS-8 FE	✓	✓	✓	✓	✓	✓

Notes: The sample is restricted to firm-product pairs for which exports to the U.S. account for more than 80 percent of total exports in columns (1)–(3) and more than 90 percent in columns (4)–(6). The dependent variable pertains to different rerouting measures. Column (1) uses an extensive-margin rerouting indicator ($Ex-Im$) that equals one if a firm imports an HS 8-digit product from China and exports the same HS 8-digit product to the US in a given quarter. Columns (2) and (3) use adjusted (RR^A) and smoothed (RR^S) measures of rerouting. *Post* is a binary indicator that equals 1 after 2018-Q2, else zero. $Treat$ is a binary indicator that equals 1 for products targeted by the 2018 US Section 301 tariffs, else zero. Regressions are at the firm × product (HS 8-digit) × quarter level. Standard errors, clustered at the HS 8-digit level, are in parentheses. ** p < 0.01, * p < 0.05, ^{+}p<0.1.

Table A.11: Robustness: Using HS 6-Digit Products as Controls

Dep. Var	Ex-Im	RR^A	RR^S
	(1)	(2)	(3)
Treat × Post	0.063**	0.037**	0.035**
	(0.017)	(0.010)	(0.010)
Observations	6389264	6389264	6389264
R-Squared	0.503	0.438	0.441
HS-6 × QnY FE	✓	✓	✓
Firm × HS-8 FE	✓	✓	✓

Notes: This table restricts the control group to HS 8-digit products within the same HS 6-digit category as treated products. The dependent variable pertains to different rerouting measures. Column (1) uses an extensive-margin rerouting indicator ($Ex-Im$) that equals one if a firm imports an HS 8-digit product from China and exports the same HS 8-digit product to the US in a given quarter. Columns (2) and (3) use adjusted (RR^A) and smoothed (RR^S) measures of rerouting. *Post* is a binary indicator that equals 1 after 2018-Q2, else zero. $Treat$ is a binary indicator that equals 1 for products targeted by the 2018 US Section 301 tariffs, else zero. Regressions are at the firm × product (HS 8-digit) × quarter level. Standard errors, clustered at the HS 8-digit level, are in parentheses. ** p < 0.01, * p < 0.05, ^{+}p<0.1.

Table A.12: Robustness: Excluding Products Targeted Under Section 232 Tariffs

Dep. Var	Ex-Im	RR^A	RR^S
	(1)	(2)	(3)
Treat × Post	0.038**	0.022**	0.021**
	(0.014)	(0.008)	(0.008)
Observations	6229692	6229692	6229692
R-Squared	0.498	0.433	0.436
Mean	0.11	0.07	0.07
HS-4 × QnY FE	✓	✓	✓
Firm × HS-8 FE	✓	✓	✓

Notes: This table is estimated on the sample that excludes Mexican products, primarily steel and aluminum, targeted by US Section 232 tariffs between 2018 and 2019. The dependent variable pertains to different rerouting measures. Column (1) uses an extensive-margin rerouting indicator ($Ex-Im$) that equals one if a firm imports an HS 8-digit product from China and exports the same HS 8-digit product to the US in a given quarter. Columns (2) and (3) use adjusted (RR^A) and smoothed (RR^S) measures of rerouting. *Post* is a binary indicator that equals 1 after 2018-Q2, else zero. $Treat$ is a binary indicator that equals 1 for products targeted by the 2018 US Section 301 tariffs, else zero. Regressions are at the firm × product (HS 8-digit) × quarter level. Standard errors, clustered at the HS 8-digit level, are in parentheses. ** p < 0.01, * p < 0.05, ^{+}p<0.1.

Table A.13: Border Proximity and Post-Period Warehouse Development

	Coefficient	(Std. Error)	T-stat	p(Radem)	p(Webb)
	(1)	(2)	(3)	(4)	(5)
Border	22.46	11.382	1.973	0.062	0.075
Post	0.80	0.576	1.395	0.125	0.212
Post × Border	12.53	5.222	2.399	0.000	0.025

Notes: The dependent variable is the quarterly number of warehouses located within each distance band (border and control) around the commercial zones of major counties handling Mexico–US exports. *Border* is an indicator for the border band, and *Post* is an indicator for the post-trade war period. All specifications absorb county fixed effects. Conventional standard errors are clustered at the county level. We report wild cluster bootstrap p-values based on the Rademacher (Radem) and Webb weight distributions, respectively, to account for the small number of clusters. The five counties in the sample and their primary ports of entry are: Dona Ana County (Santa Teresa); El Paso County (Bridge of the Americas, Ysleta-Zaragoza); Hidalgo County (McAllen-Hidalgo-Reynosa, Anzalduas, Pharr); San Diego County (San Ysidro, Otay Mesa); and Yuma County (San Luis I and San Luis II). Data source: OpenStreetMap.

Table A.14: Major Mexican Ports Used by Rerouting Firms

Mexican Port of Lading	Nearest US Port of Entry	Number of Rerouting Firms
Nuevo Laredo (MX)	Laredo	1598
Tijuana (MX)	Otay Mesa	538
Colombia (MX)	Laredo	360
Ciudad de Mexico (MX)	NA	349
Ciudad Juarez (MX)	El Paso	308

Notes: This table reports the five Mexican ports of lading used most frequently by rerouting firms during 2021–2022, together with the corresponding nearest US ports of entry. Ports are ranked by the number of unique rerouting firms. Ciudad de Mexico is an interior port in Mexico and does not have an adjacent port of entry in the US. Data are from S&P Global Panjiva.

Table A.15: Robustness: Space Rationing and Rerouting by Shipment Volume

Dep. Var	Ex-Im Pre-Period Volume		RR^A Pre-Period Volume	
Treat ×	High (1)	Low (2)	High (3)	Low (4)
2016-H1	–0.005	0.002	–0.014	0.003
	(0.009)	(0.005)	(0.009)	(0.005)
2016-H2	0.002	0.004	0.001	0.012**
	(0.014)	(0.004)	(0.012)	(0.004)
2018-H1	–0.004	0.013*	–0.003	0.015**
	(0.006)	(0.007)	(0.010)	(0.005)
2018-H2	–0.020**	0.023**	–0.008^{+}	0.014*
	(0.006)	(0.007)	(0.004)	(0.006)
2019-H1	–0.002	0.014*	–0.002	0.005
	(0.007)	(0.006)	(0.006)	(0.005)
2019-H2	–0.013*	0.010	–0.014^{+}	0.009^{+}
	(0.005)	(0.007)	(0.008)	(0.004)
2020-H1	–0.014	0.008	–0.008	0.019**
	(0.009)	(0.007)	(0.007)	(0.006)
2020-H2	–0.004	0.023*	–0.004	0.019**
	(0.007)	(0.009)	(0.006)	(0.006)
2021-H1	0.033	0.091**	0.013	0.060**
	(0.024)	(0.032)	(0.014)	(0.022)
2021-H2	0.042^{+}	0.107**	0.019	0.067**
	(0.024)	(0.034)	(0.016)	(0.023)
2022-H1	0.041^{+}	0.096**	0.017	0.061**
	(0.023)	(0.033)	(0.016)	(0.022)
2022-H2	0.037	0.103**	0.013	0.061**
	(0.023)	(0.032)	(0.013)	(0.022)
Observations	2445520	3239180	2445520	3239180
R-Squared	0.556	0.513	0.465	0.451
HS-4 × QnY FE	✓	✓	✓	✓
Firm × HS-8 FE	✓	✓	✓	✓

Notes: This table reports event-study estimates of rerouting activity, separately by pre-period shipment volume at the product level. The dependent variable in columns (1)–(2) is the extensive-margin indicator ($Ex{-}Im$) that is equal to 1 if a firm rerouted HS 8-digit product in a given quarter. Columns (3)–(4) use the adjusted (RR^A) measure. $Treat$ is a binary indicator that equals 1 for products targeted by the 2018 US Section 301 tariffs, else zero. Coefficients are reported relative to the omitted baseline year, 2017. The sample is split by pre-period shipment volume. For each HS 8-digit product, we compute the median shipment volume across all pre-period observations and classify products as High or Low depending on whether this median lies above or below the overall median across products. Regressions are at the firm × product (HS 8-digit) × quarter level. Standard errors, clustered at the HS 8-digit level, are in parentheses. ** p < 0.01, * p < 0.05, ^{+}p<0.1.

Table A.16: Robustness: Evidence for Space Rationing on Mexico–US Export Leg (Value Density)

Dep. Var	Exported			
	Value / Volume		Value / Weight	
Treat ×	High (1)	Low (2)	High (3)	Low (4)
2016-H1	0.011	–0.006	0.011	–0.006
	(0.010)	(0.022)	(0.010)	(0.022)
2016-H2	0.014	–0.001	0.015	–0.001
	(0.009)	(0.032)	(0.009)	(0.032)
2018-H1	0.002	–0.008	0.002	–0.009
	(0.009)	(0.012)	(0.009)	(0.012)
2018-H2	0.003	–0.022	0.003	–0.022
	(0.008)	(0.030)	(0.008)	(0.029)
2019-H1	0.012	–0.030	0.012	–0.026
	(0.010)	(0.032)	(0.010)	(0.033)
2019-H2	0.004	–0.055^{+}	0.003	–0.052
	(0.012)	(0.033)	(0.012)	(0.034)
2020-H1	0.010	–0.010	0.009	–0.006
	(0.012)	(0.026)	(0.012)	(0.027)
2020-H2	0.020	–0.017	0.019	–0.012
	(0.013)	(0.027)	(0.013)	(0.028)
2021-H1	0.223**	–0.096	0.226**	–0.093
	(0.056)	(0.132)	(0.056)	(0.131)
2021-H2	0.245**	–0.077	0.249**	–0.075
	(0.058)	(0.142)	(0.058)	(0.141)
2022-H1	0.241**	–0.063	0.245**	–0.060
	(0.056)	(0.148)	(0.056)	(0.147)
2022-H2	0.239**	–0.061	0.243**	–0.059
	(0.056)	(0.141)	(0.055)	(0.140)
Observations	2646672	3038140	2672040	3012828
R-Squared	0.334	0.330	0.333	0.329
HS-4 × QnY FE	✓	✓	✓	✓
Firm × HS-8 FE	✓	✓	✓	✓

Notes: This table reports event-study estimates of exporting activity to the US, separately by pre-period shipment value density at the product level. The dependent variable is an indicator equal to one if a firm exports a given HS 8-digit product from Mexico to the United States in a given quarter. *Treat* is a binary indicator that equals 1 for products targeted by the 2018 US Section 301 tariffs, else zero. Coefficients are reported relative to the omitted baseline year, 2017. In columns (1) and (2), products are split by pre-period value per unit volume: for each HS 8-digit product, we compute the median value per unit volume across all pre-period observations and classify products as High or Low depending on whether this median is above or below the overall median across products. In columns (3) and (4), products are split analogously using pre-period value per unit weight. Regressions are at the firm × product (HS 8-digit) × quarter level. Standard errors, clustered at the HS 8-digit level, are in parentheses. ** p < 0.01, * p < 0.05, ^{+}p<0.1.

Table A.17: Rerouting: Role of Prior Rerouting Experience

Dep. Var	Ex-Im		RR^A	
	Prior Rerouter		Prior Rerouter	
	Yes	No	Yes	No
	(1)	(2)	(3)	(4)
Treat × Post	0.045*	0.011**	0.027*	0.006**
	(0.018)	(0.004)	(0.011)	(0.002)
Observations	4355456	2043076	4355456	2043076
R-Squared	0.474	0.297	0.418	0.254
HS-4 × QnY FE	✓	✓	✓	✓
Firm × HS-8 FE	✓	✓	✓	✓

Notes: The dependent variable in columns (1)–(2) is the extensive-margin indicator ($Ex-Im$) that is equal to 1 if a firm rerouted HS 8-digit product in a given quarter. Columns (3)–(4) use the adjusted (RR^A) measure. Columns (1) and (3) present estimates on the subset of firms that rerouted at least one product before the trade war. Columns (2) and (4) report results on the subset of firms that did not reroute any product before the trade war. *Post* is a binary indicator that equals 1 after 2018-Q2, else zero. $Treat$ is a binary indicator that equals 1 for products targeted by the 2018 US Section 301 tariffs, else zero. Regressions are at the firm × product (HS 8-digit) × quarter level. Standard errors, clustered at the HS 8-digit level, are in parentheses. ** p < 0.01, * p < 0.05, ^{+}p<0.1.

B A Simple Model of Rerouting under Tariffs

This section presents a simple model that formalizes the mechanism by which tariffs lead firms to reroute trade through third countries.

B.1 Environment and Firm Choice

There are three locations: an origin O with producers, an intermediary M, and a destination D with consumers. At origin O, there is a unit mass of potential producers indexed by i. Products are indexed by p, and time periods are indexed by t. The destination market has inverse demand $p = a - bQ$, where Q is the aggregate demand. Each producer can supply the product p with marginal cost c_p.

If the producer i exports p directly from $O \to D$, it incurs an iceberg transport cost $t_{OD,pt}$ and a per-unit effective tariff $\tau_{pt} \geq 1$. The resulting unit cost, k^d_{pt}, for direct export to D is:

$$k^d_{pt} = c_p \, t_{OD,pt} \, \tau_{pt}. \tag{B.6}$$

Alternatively, if the producer reroutes the product through the intermediary location M, it incurs a total iceberg transport cost of $t_{OM,pt}t_{MD,pt}$, as well as an idiosyncratic iceberg rerouting factor $\chi_{ipt} \geq 1$. This χ_{ipt} captures per-unit proportional costs related to handling, coordination, compliance, and RoO at the firm–product–time level. The unit cost under rerouting is given by:

$$k^r_{ipt} = c_p \, t_{OM,pt} \, t_{MD,pt} \, \chi_{ipt}. \tag{B.7}$$

We make the following assumptions:

Assumption 1 (triangle inequality in transport cost: $t_{OM,pt}t_{MD,pt} \geq t_{OD,pt}$ for all (p,t)).

The baseline transport cost through the intermediary location is higher than or equal to direct shipment.

Assumption 2 (heterogeneity in rerouting costs). Firms differ in χ_{ipt}, which we model as

$\ln(\chi_{ipt}) = r_{ipt} = X'_{ipt}\beta + u_{ipt}$ with $u_{ipt} \sim G$ on $[0, \bar{r}]$ and density g that is continuous and positive on the interior. Here, X_{ipt} is a vector that includes firm-product level observables.[1]

Assumption 3 (competitive market in Destination D). Firms take the prices in D as given.

Firms choose rerouting over direct transport if:

$$k^r_{ipt} \leq k^d_{pt} \quad \Leftrightarrow \quad \chi_{ipt} \leq \frac{t_{OD,pt}.\tau_{pt}}{t_{OM,pt}t_{MD,pt}}. \tag{B.8}$$

We transform the above equation into logs. Let δ_{pt} define the extra transport burden of rerouting via M, given by $\delta_{pt} = \log(t_{OM,pt}t_{MD,pt}) - \log(t_{OD,pt}) \geq 0$. Then, a producer i chooses to reroute product p at time t if and only if:

$$r_{ipt} \leq \hat{\tau}_{pt} - \delta_{pt} \equiv \tilde{r}_{pt}, \tag{B.9}$$

where $\hat{\tau}_{pt} = \log(\tau_{pt})$. Hence, firms choose to reroute only when the tariff exceeds the extra transport burden. Using $r_{ipt} = X'_{ipt}\beta + u_{ipt}$ with $u_{ipt} \sim G$, we have the following rerouting indicator: $y_{ipt} = \mathbb{1}\{r_{ipt} \leq \tilde{r}_{pt}\}$. The rerouting share s_{pt} is therefore:

$$s_{pt} \equiv \mathbb{E}_i[y_{ipt}] = \mathbb{E}_i\left[G\left(\tilde{r}_{pt} - X'_{ipt}\beta\right)\right] \in [0, 1]. \tag{B.10}$$

The Equations (B.9) and (B.10) result in the following testable predictions based on the data:

Testable Prediction 1 (threshold for zero rerouting). Define $m_{pt} \equiv \inf_i X'_{ipt}\beta$. Then:

$$s_{pt} = 0 \qquad \text{whenever} \qquad \hat{\tau}_{pt} - \delta_{pt} \leq m_{pt};$$

in other words, there exists a threshold $\bar{\hat{\tau}}_{pt} \equiv \delta_{pt} + m_{pt}$ below which rerouting is absent.

Testable Prediction 2 (monotonicity of rerouting). On the interior where $g(\cdot) > 0$, the rerouting share is weakly increasing in the log tariff $\hat{\tau}_{pt}$ and weakly decreasing in the

[1] Lower r_{ipt} may reflect access to affiliates, prior trade experience, or MNC status.

rerouting transport burden δ_{pt}:

$$\frac{\partial s_{pt}}{\partial \hat{\tau}_{pt}} \geq 0, \qquad \frac{\partial s_{pt}}{\partial \delta_{pt}} \leq 0.$$

If X_{ipt} is held fixed and $g(\cdot) > 0$ everywhere on the relevant support, these inequalities are strict.

C Appendix: Other Details

C.1 Construction: Smooth Measure of Rerouting

We begin by defining value added, but now using a smooth approximation:

$$VA_{\text{smooth}} = \frac{1}{k} \log \left(1 + \exp\left(k \cdot \frac{E_{fpt} - I_{fpt}}{E_{fpt} + \epsilon}\right)\right)$$

where the parameter k governs the sharpness of the transition. The smoothed rerouting measure is then defined as:

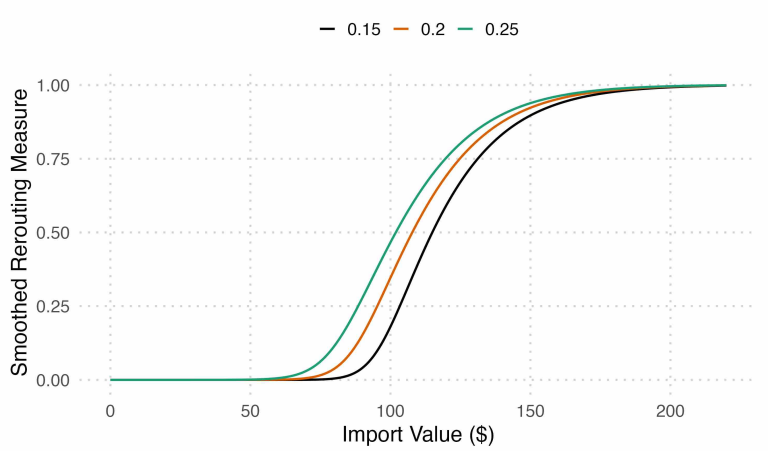
$$RR^S_{fpt} = \frac{1}{k} \log \left(1 + \exp\left(k \cdot \left(1 - \frac{VA_{\text{smooth}}}{\theta}\right)\right)\right) \times Ex - Im_{fpt}. \tag{C.11}$$

Once again, the variable θ captures the threshold for value addition, which we fix at 0.2 for our baseline regressions. Qualitatively, the behavior of RR^S_{fpt} parallels that of RR^A_{fpt}, assigning zero values for cases with high value addition. Even quantitatively, there is high agreement between these two measures for θ equals 0.2. Appendix Figure C.1 shows the measure's behavior across alternative choices of θ.

C.2 Rerouters vs. Exporters: Distance to Customs

We hand-collect geospatial data on Mexican customs offices (Appendix Figure C.2 shows these locations). On the firm side, we extract the geolocation of Mexican firms from the

Figure C.1: Variation in Smooth Rerouting Measure for Different Value Addition Thresholds



Notes: The figure gives the value of smooth rerouting measure, RR^S, for different values of θ, value addition thresholds. Parameter values: Exports to the US is 100 USD, and ϵ equals 0.1.

Panjiva dataset for all exporters to the US.[1] We link each firm's city to its nearest customs office by calculating the minimum geodesic distance (using Haversine formula) over the set of customs positions. We use these distances to compare the spatial placement of rerouters versus average exporters in Mexico.

As a first test, we report kernel density plots of the distance between firms' locations and their nearest customs ports in Appendix Figure C.3. We find that rerouters are systematically located closer to customs offices than general exporters. The distribution for rerouters is highly concentrated near zero with a right tail, indicating tighter clustering of these firms near customs offices. Exporters, by contrast, are located relatively farther from their closest customs office. Quantitatively, the mean distances from the nearest customs office are 22 kilometers for rerouters and 37 kilometers for exporters. A Kolmogorov-Smirnov (KS) test confirms that the distance distributions differ significantly between the two groups of firms.[2]

We also test this difference in a regression framework in Table C.1. The dependent variable is the log distance between a firm-product pair and its nearest customs office. Our

[1] If a firm exports or imports from multiple locations, we assign the most frequently used location as its city.

[2] The Kolmogorov-Smirnov test yielded a p-value less than 2.2e-16. The D statistic, which represents the maximum vertical difference between the empirical CDFs is 0.17.

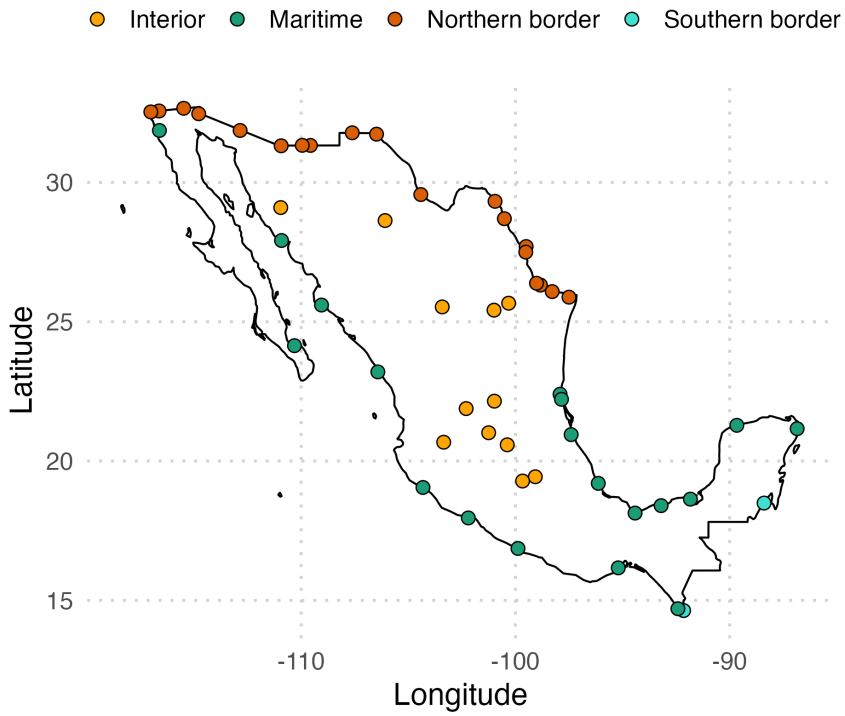
key explanatory variable, *Rerouter*, is an indicator, which is equal to one for rerouters and zero otherwise. All specifications include product fixed effects to account for product-specific geography.

In column (1), the coefficient on the rerouter indicator is negative and highly significant, indicating that rerouters are systematically located closer to customs offices. Column (2) adds controls for firm size (exports), as large exporters may have greater incentive to locate near ports to reduce transportation costs. Column (3) interacts firm size with the rerouter indicator and finds a negative interaction term, suggesting that larger rerouters locate even closer to customs offices. Quantitatively, rerouters are, on average, located approximately 50 percent closer[3] to their nearest customs post than comparable exporters.

Finally, column (4) addresses the concern of endogenous location choice after the trade war. Firms might have relocated to the border after the onset of the trade war specifically to exploit the tariff differential. To rule this out, we fix firm locations at their pre-trade war addresses and re-estimate the regression. The coefficient remains negative, significant, and quantitatively similar to the baseline. This stability implies that our results are not driven by firm relocation. Rather, rerouting was primarily adopted by firms with ex-ante geographic advantages, those for whom the marginal cost of accessing the US market was already low.

[3]A coefficient of -0.558 translates to around $100(e^{-0.692} - 1)$ =-50% change

Figure C.2: Spatial Distribution of Major Customs Offices in Mexico



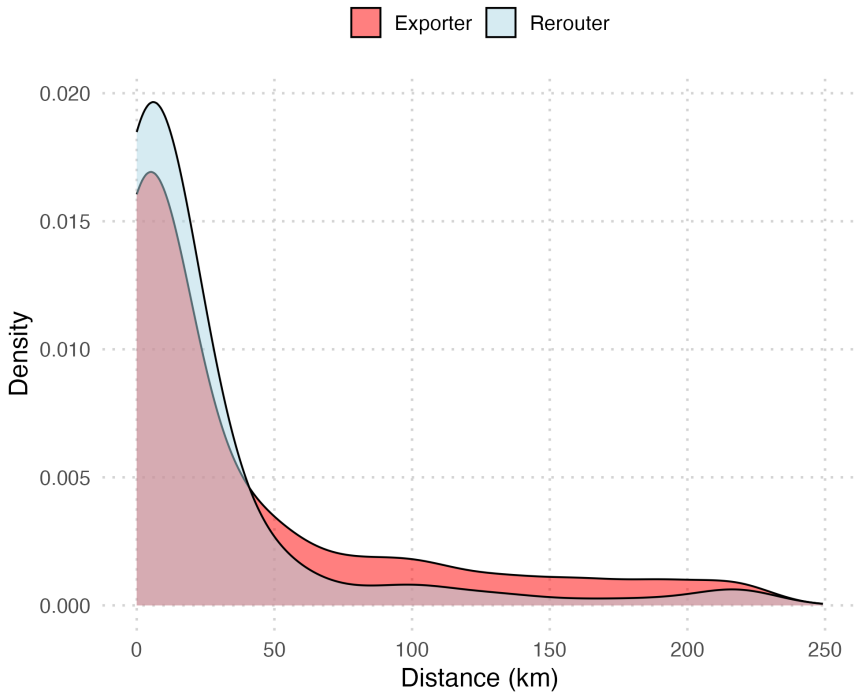
Notes: This figure shows the locations of major customs offices in Mexico, classified into four groups: northern border (red dots), southern border (blue dots), interior (black dots), and maritime (green dots).

Table C.1: Distance to the Nearest Customs Office: Rerouters vs. Other Exporters

Dep. Var	log(Distance)			
	(1)	(2)	(3)	(4)
Rerouter	–0.691**	–0.689**	–0.692**	–0.593**
	(0.010)	(0.010)	(0.029)	(0.035)
log(Exports)		0.009**	0.009**	0.017**
		(0.001)	(0.003)	(0.003)
Rerouter × log(Exports)			0.000	–0.009*
			(0.003)	(0.004)
Observations	221530	221530	221530	163199
R-Squared	0.182	0.182	0.182	0.187
Mean	1.43	1.43	1.43	1.41
HS-8 FE	✓	✓	✓	✓

Notes: The dependent variable in columns (1)–(3) is the log distance between a firm's location and its nearest customs office. In column (4), the dependent variable is the log distance in the pre-period for the same firm × product combination. Rerouters are defined as exporters with at least one positive value of the rerouting indicator, $Ex-Im$, over the entire period. log(Exports) is the natural log of the firm's average quarterly value of exports. The unit of observation is the firm × product. Each regression absorbs HS 8-digit product fixed effects. Standard errors are clustered at the HS 8-digit level. ** p < 0.01, * p < 0.05, ^{+}p<0.1.

Figure C.3: Distance to the Nearest Customs Office: Exporters and Rerouters



Notes: This figure plots the distribution of distances from firms to their nearest customs office for exporters and rerouters. Rerouters are defined as exporters with at least one positive value of the rerouting indicator, $Ex - Im$, in the pre-period. Distances, measured in kilometers, are calculated using the Haversine formula. Kolmogorov–Smirnov tests reject equality of the two distributions.